BACHELOR THESIS

OPTIMIZATION OF TEMPERATURES IN A CONDENSING CO_2 TO METHANOL REACTOR

JORRIT KROES

FACULTY OF SCIENCE AND TECHNOLOGY
CHEMICAL ENGINEERING
SUSTAINABLE PROCESS TECHNOLOGY

EXAMINATION COMMITTEE
PROF. DR. A.J.A. WINNUBST
DR. IR. D.W.F. BRILMAN
M.J. BOS MSc.

UNIVERSITY OF TWENTE.

26 JANUARY 2015

Abstract

In this study, the effect of the catalyst temperature on the productivity, as well as the energy efficiency under natural and low forced convection, in a condensing CO_2 to methanol reactor, is investigated in order to find the optimal catalyst temperature. For both cases, the pressure in the reactor and the condenser outlet gas temperature is kept constant at 50bar and 373K respectively. To predict at which catalyst temperature the productivity is the highest at a condenser outlet temperature of 373K, a kinetic model over the catalyst bed and a phase equilibrium model for the condenser of the experimental reactor setup are developed. The experimental results show that the productivity for both, forced and natural convection, is the highest at a catalyst out temperature of 502K. At higher catalyst temperatures, the productivity remains at a constant level. Because of this the reactor setup is limited by the condenser. Due to the fact that the reactor setup is limited by the condenser, the highest energy efficiency for forced and natural convection is found at the same temperature of 502K. Therefore, the catalyst temperature of 502K is identified as the optimal catalyst temperature by a condenser outlet gas temperature of 373K.

Table of contents

1. Introduction

The fossil fuel reserves on earth are finite and strongly decreasing due to intensive consumption [1, 2]. In addition to that, the remaining reserves become harder to exploit and thereby increasing the costs of fossil fuel. However, most of the electricity today is still generated by burning fossil fuels. The combustion of fossil fuel releases carbon dioxide (CO_2) [2]. CO_2 is a major greenhouse gas and is a harmful contamination of the atmosphere that causes global warming. This is why more and more electricity is produced in a sustainable way, for example by solar, wind and geothermal energy [1]. An occurring problem of electricity is that the transportation and storage is difficult. Next to this, the ratio of supply and demand of electricity is not in balance at certain times on a day and during the seasons in a year [2]. Therefore, a suitable storage medium is needed in which electricity can be stored. One of the potential storage media is methanol (CH_3OH) [1].

Methanol is a liquid and can easily be stored in tanks and transported by trucks, ships and pipelines [3]. Moreover, methanol can be entirely produced in a sustainable way. The electricity from renewable sources [4] which is not consumed in the electricity grid can be used for the electrolyses of water to produce hydrogen (H_2). The hydrogen can be converted with CO_2 in a catalyzed direct hydrogenation reaction to methanol [2]. The advantage of methanol is its versatility. It can be easily converted back to electricity by a direct methanol fuel cell (DMFC) or combustion, used as a replacement for gasoline and upgraded into a diesel substituent (DME). It is also an important feedstock for other chemical products as formaldehyde, methyl tert-butyl ether (MTBE), acetic acid, methyl methacrylate (MMA) and dimethyl terephthalate (DMT) [3, 5]. Light olefins such as ethylene and propylene, which are used for the manufacturing of polymers and hydrocarbon fuels, are produced using the methanol-to-olefins (MTO) process[6].

A new reactor setup has been developed for the catalytic direct hydrogenation reaction. The reactor consists of two temperature zones: one zone with high temperature for production of methanol from the gaseous reactants and another zone with a lower temperature for condensation of the vapor products. The reactor operates in a so called Gas-In, Liquid-Out mode of operation because only liquid phase products are removed from the reactor [7]. Current research on this new rector concept focuses on understanding the system and finding the operational limitations and the optimal reaction conditions. This is why additional experimental research is needed on the optimum temperature levels inside the reactor in order to find the optimal reaction temperature.

To find the optimal reaction temperature, the temperature effect on the reactor productivity is studied at constant low condenser temperature and constant low fan speed. In order to investigate to what extent the outcome of the temperature effect holds for gas circulation under natural convection conditions, the fan is turned off and the study is repeated under the same conditions. The experimental results are then compared with an equilibrium based reactor model. Due to the fact that renewable electricity is stored in methanol the energy efficiency of this reactor plays also an important role. The research question for this bachelor assignment is therefore:

What is the optimal catalyst temperature for this new reactor set up at a constant condenser temperature to store renewable electricity into methanol in an energy efficient way?

2. Literature review

In this chapter an overview of the literature for the production of methanol is given. First, the current industrial methanol production from syngas is introduced, followed by an alternative production route, the catalytic hydrogenation of carbon dioxide with hydrogen. Then, occurring problems with respect to thermodynamic equilibrium and catalyst degradation are discussed. In that regard, a new reactor set up is introduced as a solution to shift the thermodynamic equilibrium. This chapter ends with a comparison of CO_2 and CO based reaction kinetics for the methanol production.

2.1. Industrial methanol production

Currently, methanol is industrially produced from fossil fuel based syngas. Syngas is a mixture of hydrogen and carbon monoxide (CO), as well as CO_2 produced from partial combustion of coal or steam reforming of natural gas over a heterogeneous catalyst [1, 3, 5]. Especially the production of syngas from coal generates large amounts of CO_2 as a byproduct which causes environmental problems because CO_2 is a significant greenhouse gas and is considered as a harmful pollutant of our atmosphere and a major source for human caused global warming. Because of this problem, the major source for syngas production became natural gas which is more convenient, economic, and environmentally friendly to use [1]. Today, steam reforming is the technology most widely used to produce syngas from natural gas (equation 1). The combination of methane steam reforming with partial oxidation (equation 2) is called autothermal reforming and is also widely used in processes [1, 3, 5]. A third process called dry reforming (equation 3) is also used to produce syngas however in a lesser extent than the first two options [1].

$$CH_4 + H_2O \rightleftharpoons CO + 3\,H_2 \qquad (1)$$

$$CH_4 + 0.5\,O_2 \rightleftharpoons CO + 2\,H_2 \qquad (2)$$

$$CH_4 + CO_2 \rightleftharpoons 2\,CO + 2\,H_2 \qquad (3)$$

Alternatively, syngas can be produced from CO_2 and water (H_2O). Since the amount of oxygen in methanol is lower than in the sum of the amount of oxygen in H_2O and CO_2, oxygen has to be removed somewhere in the process. This can be achieved in three ways: by deoxygenation of CO_2 (equation 4), by deoxygenation of H_2O (equation 5) and by deoxygenation of both components [7].

$$CO_2 \rightleftharpoons CO + 0.5\,O_2 \qquad \Delta H_{298K} = 283\ kJ/mole \qquad (4)$$

$$H_2O \rightleftharpoons H_2 + 0.5\,O_2 \qquad \Delta H_{298K} = 286\ kJ/mole \qquad (5)$$

The minimum required energy to remove oxygen from either CO_2 or water is the enthalpy of the reaction. This energy is equal for both reactions, as can be seen in equations 4 and 5. However, it is experimentally proven that the conversion of CO_2 to CO has a low efficiency with the current state of technology, whereas the required hydrogen can be produced with high efficiency via electrolysis [4].

By adjusting the CO:H_2 ratio close to 1:2 the syngas can be converted into methanol (equation 6). Present processes use copper (Cu)/zinc oxide (ZnO) based catalysts which are extremely active and selective in heterogeneous gas phase processes [1, 3, 5].

$$CO + 2\,H_2 \rightleftharpoons CH_3OH \qquad \Delta H_{298K} = -90.8\ kJ/mole \qquad (6)$$

By current industrial technology a one pass a carbon conversion of only 50% to 80% can be achieved, depending on the synthesis gas composition and the selected process. Therefore, after methanol and water are condensed and removed, the remaining gas must be recycled to the reactor. The exothermic formation of methanol takes place in the reactor at 473 – 573K and pressures of 100 – 250bar [3, 5]. The chemical equilibrium yield at different pressures is shown in Figure 1.

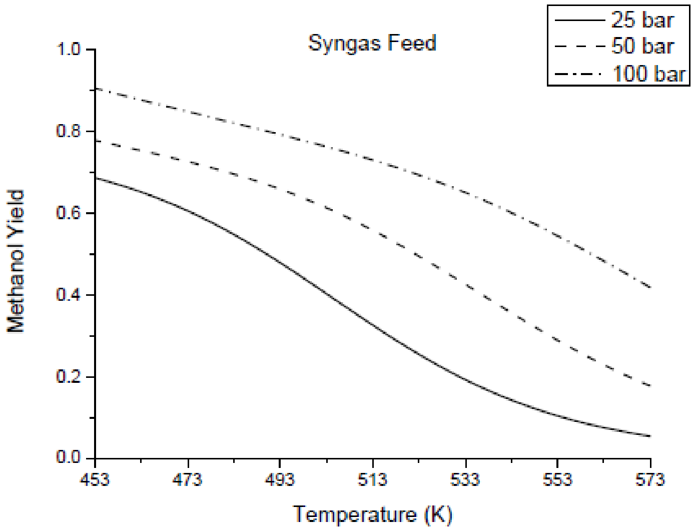

Figure 1: Chemical equilibria in methanol synthesis from syngas at different pressures. Syngas feed: $H_2/CO/CO_2$ 75.9/16.9/7.2 [7].

2.2. Catalytic hydrogenation of carbon dioxide

A simple, alternative way to produce methanol is the direct catalytic hydrogenation of CO_2 with hydrogen (equation 7). This reaction has been recognized as one of the most promising process to stabilize the atmospheric content of carbon dioxide because of a large demand for methanol as fuel and basic chemical [1]. Both homogeneous and heterogeneous catalysts have been studied for the hydrogenation of CO_2. With respect to cost, stability, separation, handling and reuse of the catalyst, as well as reactor design, a heterogeneous catalyst is favored [2]. The main products of the hydrogenation reaction are methanol, CO and water, as can be seen in the equations 7 and 8 below [7].

$$CO_2 + 3H_2 \rightleftharpoons CH_3OH + H_2O \qquad \Delta H_{298K} = -49.2\ kJ/mole \qquad (7)$$

$$CO_2 + H_2 \rightleftharpoons CO + H_2O \qquad \Delta H_{298K} = 41.6\ kJ/mole \qquad (8)$$

Efficient catalysts based on metals and their oxides have been developed for this reaction. It has been shown that Cu/ZnO based catalysts are the most useful systems for the catalytic hydrogenation of CO_2 to methanol [8]. In order to increase the stability and the activity of the catalyst aluminum oxide (Al_2O_3) is used as the promoter to disperse the Cu and ZnO [8]. Because the catalyst is similar as the one used in the industrial process, the exothermic formation of methanol takes place at the same temperature range of 473 – 573K in the reactor. The chemical equilibrium yield at different pressures is shown in Figure 2.

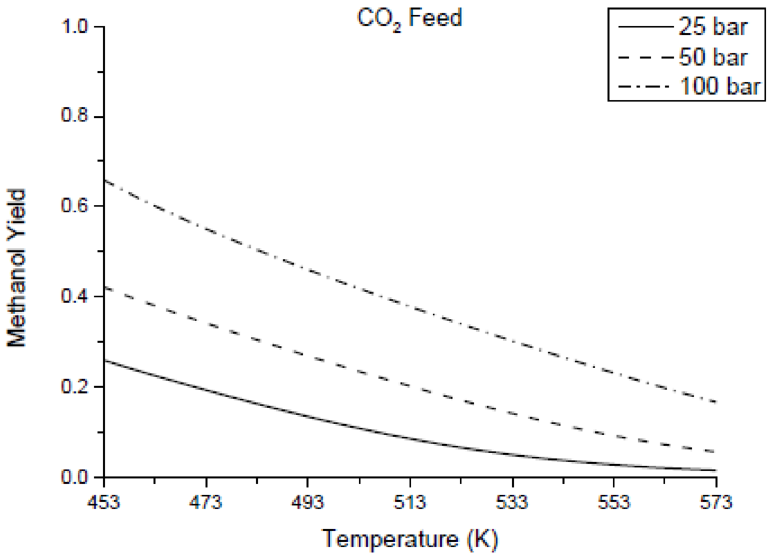

Figure 2: Chemical equilibria in methanol synthesis from CO_2 at different pressures. CO_2 feed: $H_2/CO/CO_2$ 75.0/0/25.0 [7].

2.3. Reactor design

The direct hydrogenation reaction introduced in the previous chapter discloses one problem: The equilibrium conversion of the CO_2 /H_2 mixture is low, as can be seen in Figure 2. To solve this problem, a new reactor set up has been developed. This reactor has two temperature zones: a high and a low temperature zone, to shift the chemical equilibrium to the product side by product vapor condensation. In the high temperature zone, the catalyst operates and the reactants are converted in the gas phase. In the low temperature zone, the temperature is lowered below the dew point temperature of the products to condensate them in-situ. In this setup, the cold temperature zone (condenser) is placed on top of the hot temperature zone (catalyst) to benefit from natural convection flow. However, a fan is installed in order to ensure optimal reactor performance.

The reactor operates in a Gas-In, Liquid-Out mode because only products in the liquid phase are removed from the reactor. This secures that, full conversion of the gas phase reactants, H_2 and CO_2, to the liquid phase products, methanol and water can be achieved. Due to this full gas conversion there is no need for an external recycle of reactants. Furthermore, this concept eliminates possible carbon selectivity loss to CO in the reaction zone because CO will not leave the reactor as long as it is in the gas phase [7].

The condenser performance improves when the condenser temperature is lowered. Calculations have shown that a low condenser temperature increases the single-pass conversion [7]. The optimal reaction temperature is a balance between, on the one hand, the more optimal thermodynamic equilibrium at low temperature, since the reaction is exothermic, and on the other hand, faster kinetics at high temperature because the reaction rate constant is high this way [9].

2.4. Catalyst degradation

Copper based catalysts are sensitive to deactivation factors like temperature and poisoning. The $Cu/ZnO/Al_2O_3$ catalyst can operate in the temperature range from 473K to 573K as mentioned earlier. If the temperature exceeds the temperature range, sintering and agglomeration of Cu and ZnO can easily occur, resulting in a smaller active surface area and therefore, decreasing the activity [3, 5]. Deactivation caused by poisonous compounds is rarely a problem in methanol production because poisonous sulfur and halide components are effectively removed in feed pretreatment [3, 10]. Nevertheless, water has an influence on the performance of the catalyst.

As mentioned in chapter 2.2., an equivalent amount of water is produced during the hydrogenation of CO_2 (equation 7) [8]. A third of the H_2 is converted into water, which is much higher than that converted during the industrial production of methanol from syngas [6]. The produced water has a crucial effect on the activity and performance of the catalyst. Due to strong competitive adsorption, water occupies and blocks the active sites on the catalyst surface area causing fewer sites for CO_2 to bond. Furthermore, it is known that water is a strong oxidant for metals as Cu [8]. For this reason, the active sites of the $Cu/ZnO/Al_2O_3$ catalyst are oxidized and consequently, it loses its activity. The oxidized Cu sites can be reduced back by hydrogen or CO gas. However, when the reduction rate is too low, which means that the partial pressure of water is higher than the partial pressures of hydrogen and CO, most of the active sites remain oxidized so that the activity of the catalyst is lost [8].

Wu et al. [11] studied the stability of Cu/ZnO based catalysts in the methanol synthesis from a CO_2 and CO rich feed respectively. At a CO rich feed no significant water is formed, as is shown in Figure 3. This is consistent with equation 6. However, when the amount of CO_2 in the feed is increased, water is formed as expected by equation 7. The formed water accelerates the crystallization of Cu and ZnO in the catalyst which leads to faster sintering and associated deactivation of the catalyst surface [2, 6, 11].

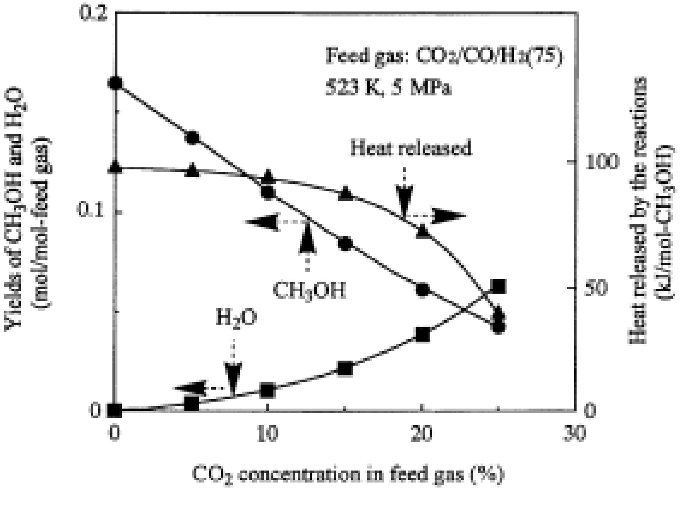

Figure 3: Yields of methanol / water and heat released at equilibrium in methanol synthesis as a function of CO_2 concentration in the feed gas [11].

This inhibitory effect of water on the methanol synthesis was also observed by Saito et al. [12]. The presence of water in the reactor suppressed the methanol synthesis over Cu/ZnO based catalysts, resulting in a lower methanol yield and relative reaction rate [12], as can be seen in Figure 3 and Figure 4 respectively. In Figure 4, r_0 and r represents the rates of methanol synthesis or CO formation without (pure CO_2) and with the addition of H_2O or CO respectively [12]. It can be seen that the relative reaction rate of methanol decreases with increasing water partial pressure.

Saito et al. [12] studied also the activity of Cu/ZnO based catalyst on different support materials as Al_2O_3, ZrO_2 and SiO_2 for the methanol synthesis from CO_2 and H_2. They found that multi-component catalysts as $Cu/ZnO/ZrO_2/Al_2O_3$ and $Cu/ZnO/ZrO_2/Al_2O_3/Ga_2O_3$ are more active and stable than bi- or ternary catalysts because they have a higher surface area, basicity, and thermal stability. Furthermore, Wu et al. [11] found that the addition of a small amount of colloidal silica to the multi-component catalysts vastly improved the long-term stability.

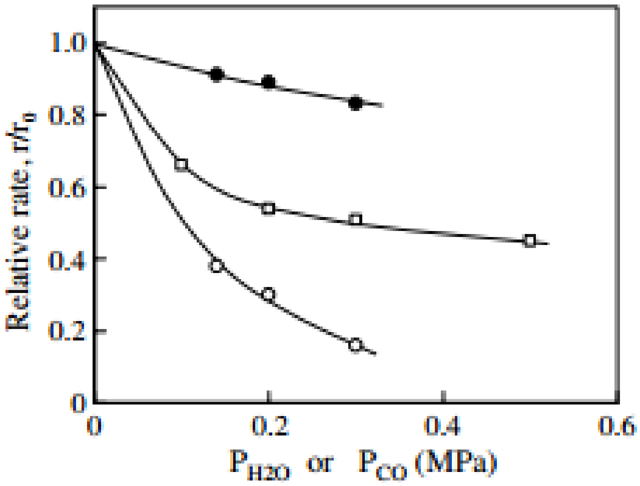

Figure 4: Inhibitory effects of H2O (o) and CO (□) on methanol synthesis and of H2O (•) on CO formation from CO2(25%)/H2(75%) mixture over a Cu/ZnO/ZrO2 catalyst at 523 K [12].

Li et al. [8] investigated the performance and influence of water on three different Cu/ZnO based catalysts, namely, $Cu/ZnO/ZrO_2/Al_2O_3$ (CZZA), $Cu/ZnO/ZrO_2$ (CZZ) and $Cu/ZnO/Al_2O_3$ (CZA). The experimental results are shown in Figure 5. When no water is added, it can be seen that the conversion of CO_2 and the methanol yield is higher on the CZZA catalyst compared to the CZA and CZZ catalysts. The selectivity of methanol on CZZA is 17.3% higher than that on CZA and 11.7% higher than that on CZZ [8].

To investigate the influence of water on the catalysts, water is added in the feed stream. As the amount of water is increased, the conversion of CO_2 and methanol yield decreases, as can be seen in Figure 5. From this figure it also follows that the CZZA catalyst is proved to be the most resistant against the influence of water and that the suppressive effect of water is most remarkable for CZA.

ZrO_2 has thus a promotional effect on the catalyst performance. It promotes the catalytic activity of methanol synthesis from CO_2 and suppresses the inhibitive effect of water for the reaction as well as the catalyst deactivation [8]. Furthermore, it is noted that the catalytic activity of Al_2O_3-ZrO_2 promoted catalysts show better catalytic properties than the catalyst supported on either Al_2O_3 or ZrO_2 alone. This is due to higher Cu dispersion in the Al_2O_3-ZrO_2 promoted catalyst, resulting in a larger reactive surface area and therefore, a higher activity [8, 13].

Because of the forward and reverse water gas shift reaction (equation 8), which takes place in the presence of the Cu/ZnO based catalyst, it is difficult to separate the roles of water and CO_2 for the reaction to methanol, as can be seen in the equations 7 and 8 in chapter 2.2.

As described above, the effect of water on catalyst degradation is being discussed in literature. On the one hand, water has a degradation effect on the catalyst due to the fact that an increase in water concentration decreases the methanol reaction rate and CO_2 conversion because water blocks active sites on the catalyst surface and causes Cu crystallization. Yet, on the other hand, water has a promotional effect because it enhances the reaction rate of the forward water gas shift reaction (equation 8), so that the amount of CO in the reactor is reduced, as can be seen in Figure 5. This results in an increase of the CO_2 amount in the reactor which leads to an increase in the methanol reaction rate, even under the case of serious deactivation [8].

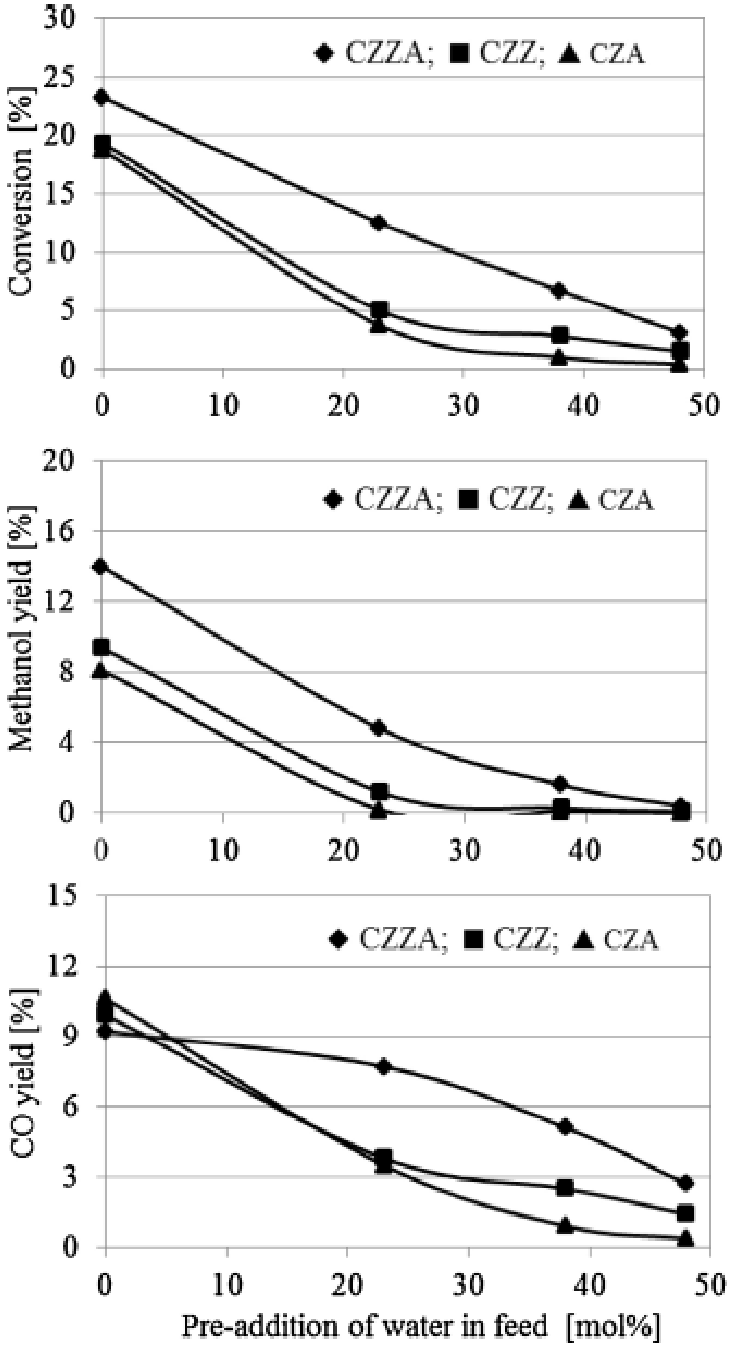

Figure 5: Influence of pre-addition of water on the CO_2 conversion, methanol yield and CO yield [8].

2.5. Comparison of CO and CO_2 based reaction kinetics

As discussed in the previous chapters, methanol can be produced from syngas (equation 6) and via catalytic direct hydrogenation (equation 7). Both reactions are exothermic and are affected by the water gas shift reaction (equation 8). Due to the exothermic character and the decrease of the number of moles during these reactions, the equilibrium is more favorable at high pressure and low temperature [7]. The calculated equilibrium methanol yield of syngas is significantly higher than of CO_2 based feed systems, as shown in Figure 1 and Figure 2 [7].

Lee et al. [14] have studied the methanol syntheses from a CO_2/H_2 and CO/H_2 feed over a $Cu/ZnO/Al_2O_3$ catalyst and compared the experimental results of the pure feeds with each other and with $CO/CO_2/H_2$ feed mixtures with a varying CO/CO_2 ratio and a fixed amount of hydrogen of 80mole%. Whereas the thermodynamic equilibrium yields are decreasing with increasing temperature, the found experimental kinetic methanol yields show a maximum for both cases, as can be seen in Figure 6. In this figure, the equilibrium and experimental kinetic methanol yields depending on temperature are shown. In contrast to the calculated equilibrium yields, the experimental kinetic yields for the CO_2 based reaction are higher than the CO based one for temperatures below 573K [14]. It is striking that the methanol yield at temperatures below 523K is one order in magnitude higher for a CO_2/H_2 than a CO/H_2 feed. The methanol yields decrease above 648K, with increasing the temperature because the product composition shifts from methanol rich to CO rich mixtures. Thereby, the carbon conversion to methanol is decreased [9].

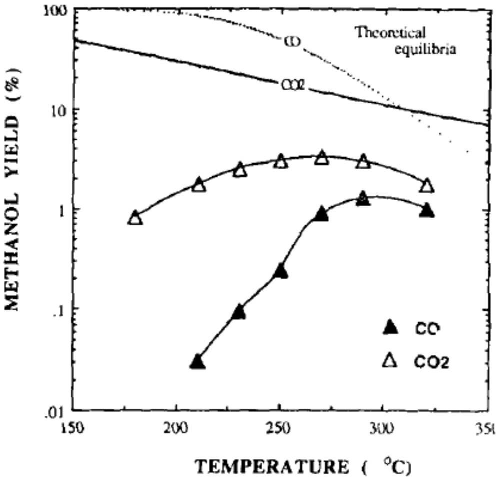

Figure 6: Calculated equilibrium and experimental kinetic methanol yields for CO/H_2 and CO_2/H_2 depending on temperature [14].

Space velocity is also an important factor that affects the methanol synthesis kinetics [10]. The space velocity is the quotient of the entering volumetric flow rate of the reactants divided by the reactor volume and reflects the reactor efficiency. In this case, the reactor volume is the catalyst bed volume. It indicates how many reactor volumes of feed can be treated in a unit of time. A higher space velocity thus means a shorter residence time [15]. Therefore, an increase in space velocity can decrease the rate of conversion.

An et al. [15] and Li et al. [8] investigated the effect of space velocity on the conversion of CO_2 and methanol yield of a CO_2/H_2 mixture with a ratio of 3. They found out that the CO_2 conversion and methanol yield decreases with an increase of space velocity. The shorter residence time caused a decrease in CO_2 conversion. The rate of reverse water gas shift reaction is much faster than the methanol synthesis reaction, so that a higher space velocity had less effect on the reverse water shift reaction than on the methanol synthesis. Therefore, the methanol yield decreases [8, 16].

Lee et al. [14] and Sahibzada et al. [16] observed that the space velocity has a different effect on the CO and CO_2 based reactions. Figure 7 shows these differences. In the CO based reaction, the CO conversion decreases rapidly with increasing space velocity while the methanol selectivity remains unchanged. In the CO_2 based reaction, the CO_2 conversion decreases much slower and the methanol selectivity increases due to the rapid decrease of CO [14]. At high space velocity, methanol production is greater with the CO_2/H_2 based reaction because the methanol production rate is greater than the CO production rate. However, at lower space velocity, methanol production is greater with CO/H_2 based reaction because the selectivity in the CO_2/H_2 based reaction switched in favor of CO. At even lower space velocity, CO production approaches equilibrium [16].

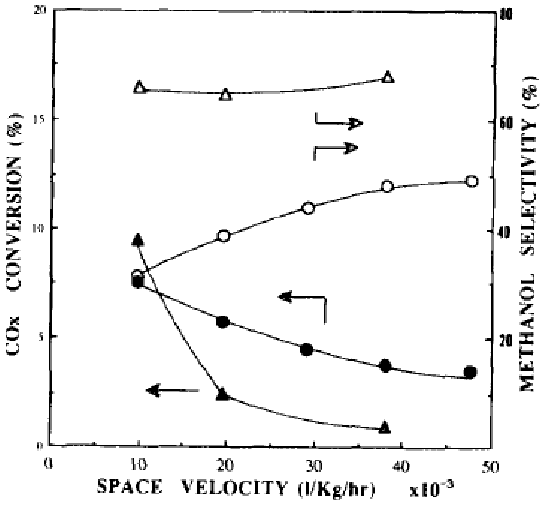

Figure 7: Effect of space velocity on carbon conversion and methanol selectivity from CO_2/H_2 (o,•) and CO/H_2 (Δ,♦)[14].

As discussed earlier, methanol is industrially produced from syngas. Syngas is a mixture of CO, CO_2 and H_2. Zhang et al. [17] discovered that both methanol production rates, of the CO and CO_2 based reactions, are much lower than the rate of syngas with a composition of $CO/CO_2/H_2$ mixture of 20.5/5/74.5, as can be seen in Figure 8.

Sahibzada et al. [16] and Lee et al. [14] both studied the effect on the reaction rate of the CO_2 concentration in the syngas. Whereas Sahibzada only studied the effects at low space velocity, Lee studied the effects at both, low and high, space velocities. Regarding low space velocity, both reached the same results. Figure 9 shows the methanol yield dependent on CO_2 concentration. At low space velocity, the methanol yield sharply increases with a small increase in CO_2 concentration, until it reached a maximum at 2-5% CO_2. A further increase in CO_2 concentration decreases the methanol production. At high space velocities, the methanol yield increases almost linearly with CO_2 concentration. It is notable that the higher the space velocity, the lower is the methanol yield is. The concentration of CO_2 in the syngas mixture has thus a determining role. High concentrations of CO_2 push the equilibrium towards an unfavorable thermodynamic regime causing low methanol yields.

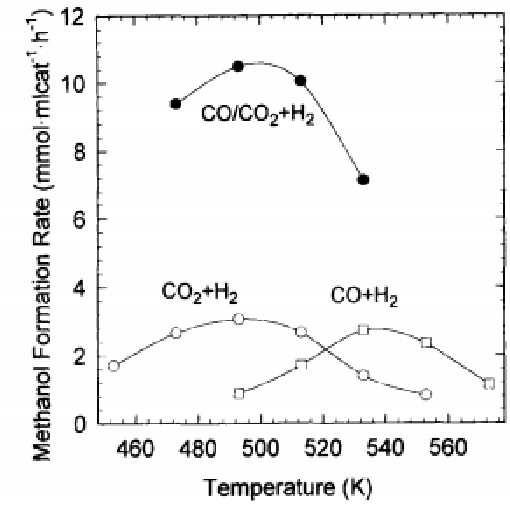

Figure 8: Methanol synthesis rate for CO/H2, CO_2/H_2 and CO (20.5)/CO_2 (5)/H_2 (74.5) [17].

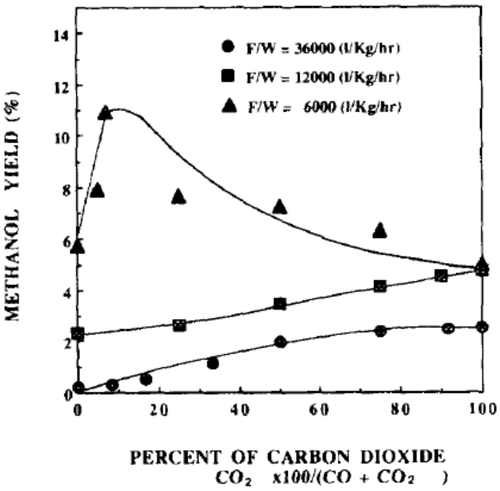

Figure 9: Methanol yields depending on CO_2 concentration at different space velocities [14].

Furthermore, the amount of water increases with increasing CO_2 concentration, as discussed in the previous chapter, leading to inhibition of the CO_2 hydrogenation. Nevertheless, operating at pure CO conditions does not result in high methanol yields either due to kinetic reasons. In order to reach a maximum conversion, an amount of CO_2 related to the ratio $(H_2-CO_2):(CO+CO_2) \approx 2$ is crucial in the feed [18]. Whereas the promotional effect of CO_2 is related to the water gas shift reaction, the deactivation at higher concentrations of CO_2 is related to the oxygen surface coverage, resulting in a decrease in Cu dispersion which is harmful for the CO_2 hydrogenation [14, 18].

Since research on the methanol synthesis from hydrogenation of CO_2 is performed under unequal conditions, such as different reactor set-ups and catalysts, there are no general reaction rate equations available. Most kinetic data is obtained from activity measurements. The reaction constants are determined with the data obtained from such activity measurements. However, it is important to set up kinetic equations for CO_2 hydrogenation in order to develop a high-efficiency reactor for methanol synthesis from CO_2 and hydrogen. Although many kinetic mechanisms have been suggested for the synthesis of methanol and water, the exact mechanism is not clearly discussed. Lim et al. [13], An et al. [15] and Skrzypek et al. [19] reviewed a couple of these mechanisms. A common used standard kinetic mechanism for process simulations is that of Graaf et al. [3] and is also used in the studies of Lim et al. [13] and Rahimpour et al. [20].

Graaf et al. considered both the hydrogenation of CO (equation 6), CO_2 (equation 7) and the water gas shift reaction (equation 8) and proposed a dual site mechanism, with CO and CO_2 adsorbing on a s1 type site and H_2 and water adsorbing on a s2 type site [13]. The methanol production from CO and CO_2 occurs via consecutive hydrogenations, while the water gas shift reaction proceeds along a formate route. Assuming adsorption and desorption to be in equilibrium, and taking every elementary step in each of the three overall reactions in turn as rate determining, Graaf et al. examined 48 possible models [13]. In order to reach the final set of kinetics, Graaf et al. used statistical discrimination [21].

The resulting reaction rate equations can be seen in equations 9 – 11.

$$r_{CO} = \frac{k_1 K_{CO}(f_{CO} f_{H2}^{3/2} - f_{CH3OH}/f_{H2}^{1/2} K_{p1})}{(1+K_{CO} f_{CO} + K_{CO2} f_{CO2})[f_{H2}^{1/2} + (K_{H2O}/K_{H2}^{1/2}) f_{H2O}]} \tag{9}$$

$$r_{CO2} = \frac{k_2 K_{CO2}(f_{CO2} f_{H2}^{3/2} - f_{CH3OH} f_{H2O}/f_{H2}^{3/2} K_{p2})}{(1+K_{CO} f_{CO} + K_{CO2} f_{CO2})[f_{H2}^{1/2} + (K_{H2O}/K_{H2}^{1/2}) f_{H2O}]} \tag{10}$$

$$r_{RWGS} = \frac{k_3 K_{CO2}(f_{CO2} f_{H2} - f_{H2O} f_{CO}/K_{p3})}{(1+K_{CO} f_{CO} + K_{CO2} f_{CO2})[f_{H2}^{1/2} + (K_{H2O}/K_{H2}^{1/2}) f_{H2O}]} \tag{11}$$

In these rate equations, K_{P1}, K_{P2} and K_{P3} are the following pseudo equilibrium constants,

$$K_{P1} = 10^{(5139/T - 12.621)} \tag{12}$$

$$K_{P2} = 10^{(3066/T - 10.592)} \tag{13}$$

$$K_{P3} = 10^{(-2073/T + 2.029)} \tag{14}$$

K_{CO}, K_{CO2} *and* $K_{H2O}/K_{H2}^{0.5}$ are the adsorption equilibrium constants of CO, CO_2, H_2O and H_2,

$$K_{CO} = (2.16E-5) * exp(\frac{46800}{RT}) \tag{15}$$

$$K_{CO2} = (7.05E-7) * exp(\frac{61700}{RT}) \tag{16}$$

$$K_{H2O}/K_{H2}^{0,5} = (6.37E-9) * exp(\frac{84000}{RT}) \tag{17}$$

and k_1, k_2, and k_3 are the rate constants of each individual reaction determined by Graaf et al. [22].

$$k_1 = (4.89E7) * exp(\frac{-113000}{RT}) \tag{18}$$

$$k_2 = (1.09E5) * exp(\frac{-87500}{RT}) \tag{19}$$

$$k_3 = (9.64E11) * exp(\frac{-152900}{RT}) \tag{20}$$

The fugacity f of the components in the gas phase is calculated from the fugacity coefficients which can be obtained from the modified Soave-Redlich-Kwong (mSRK) equation of state (equation 21) for the three reactions [23].

$$P = \frac{RT}{V-b} - \frac{a(T)}{V(V+b)} \tag{21}$$

In literature, the reaction kinetics of the methanol synthesis from CO_2 and CO as well as syngas based reactions is extensively studied. Results, however, vary with different reactor set-up, the used catalyst and applied kinetic mechanism model, making it hard to compare the results. A common used standard kinetic mechanism for process simulations is that of Graaf et al. [21]. Experimental kinetic data obtained from activity measurements is used to determine the reaction rate constants from the reactor set-up. Therefore, the kinetic mechanism model of Graaf et al. [21] is used to model the reactor and find the equilibrium and kinetic based optimal catalyst temperature, at which the productivity and energy efficiency is the highest, while the temperature of the condenser remains constant. The development and implementation of the model is discussed in the next chapter.

3. Reactor model

A kinetic model over the catalyst bed and a phase equilibrium model for the condenser of the experimental reactor setup are being developed in order to predict at which catalyst temperature the productivity is the highest at a specific fixed condenser outlet temperature. The block scheme of this model is presented in Figure 10. In this chapter the model will be described.

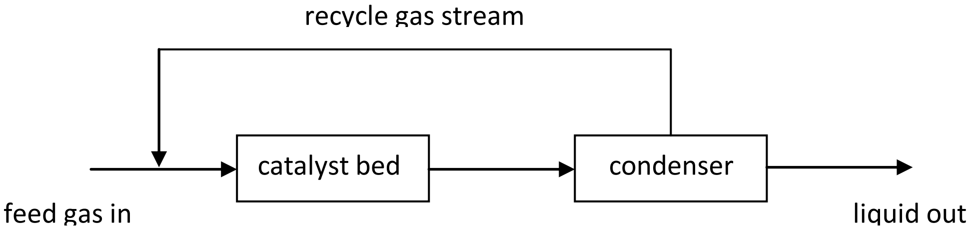

Figure 10: Block scheme of the model

3.1. Catalyst bed

The model is based on the steady state mass balance of the components over the catalyst bed. In order to simplify the model the following assumptions have been made: Firstly, the temperature and pressure are constant over the catalyst bed as well as in the catalyst pallet. Furthermore, it is assumed that the mass flow over the catalyst bed is constant. Secondly, catalyst deactivation and side reactions to higher alcohols and simple carboxylic acids are neglected. With these assumptions the general the mass balance over the catalyst bed is defined as: *Accumulation = in - out + production*. From this definition the following general equation is derived:

$$\frac{dm_j}{dt} = (\phi_m * w_j)_{in} - (\phi_m * w_j)_{out} + R_j * M_j * V_r \qquad (22)$$

In this equation *m* denotes the mass of component *j*, ϕ_m the mass flow through the catalyst bed, *w* the weight fraction of component *j*, *R* the reaction rate equation of component *j*, *M* the molar mass of component *j* and V_r the reactor volume. Since the weight fractions of the components vary over the length of the catalyst bed, a differential mass balance is needed. In the differential equation the volume of the reactor, V_r is expressed as A_r*dz. Herein, A_r denotes the cross section area of the catalyst bed and *dz* the length of the catalyst bed. The resulting differential mass equation is as follows:

$$\frac{dm_j}{dt} = (\phi_m * w_j)_z - (\phi_m * w_j)_{z+dz} + R_j * M_j * (A_r * dz) \qquad (23)$$

Since the reactor operates at steady state, there is no accumulation of mass in the reactor. From this it follows that $dm_j/dt=0$:

$$0 = (\phi_m * w_j)_z - (\phi_m * w_j)_{z+dz} + R_j * M_j * (A_r * dz) \qquad (24)$$

Dividing by dz and taking the limit of dz→0 leads to the following equation:

$$0 = \frac{-d(\phi_m * w_j)}{dz} + R_j * M_j * A_r \qquad (25)$$

The mass flow over the catalyst bed is independent of changes in the weight fractions of the components. Hence, it can be put out of the differential equation:

$$0 = -\phi_m * \frac{dw_j}{dz} + R_j * M_j * A_r \tag{26}$$

Rewriting this equation results in the final differential mass equation for component j:

$$\frac{dw_j}{dz} = R_j * M_j * \frac{A_r}{\phi_m} \tag{27}$$

It has been shown in the literature review that three reactions are involved in the production of methanol. Methanol is produced from syngas (equation 6) and by catalytic hydrogenation of CO_2 (equation 7). During the catalytic hydrogenation the reverse water gas shift reaction (equation 8) occurs as a side reaction. In these three reactions five components are present, namely CO, CO_2, MeOH, H_2 and H_2O. Therefore, five differential equations are needed to calculate the weight fractions of the components at the end of the catalyst bed. The differential equations for the five components are listed below:

$$\frac{dw_{CO}}{dz} = (-r_{CO} + r_{RWGS}) * M_{CO} * \frac{A_r}{\phi_m} * V_{cat} \tag{28}$$

$$\frac{dw_{CO2}}{dz} = (-r_{CO2} - r_{RWGS}) * M_{CO2} * \frac{A_r}{\phi_m} * V_{cat} \tag{29}$$

$$\frac{dw_{MeOH}}{dz} = (r_{CO} + r_{CO2}) * M_{MeOH} * \frac{A_r}{\phi_m} * V_{cat} \tag{30}$$

$$\frac{dw_{H2}}{dz} = (-2r_{CO} - 3r_{CO2} - r_{RWGS}) * M_{H2} * \frac{A_r}{\phi_m} * V_{cat} \tag{31}$$

$$\frac{dw_{H2O}}{dz} = (r_{CO2} + r_{RWGS}) * M_{H2O} * \frac{A_r}{\phi_m} * V_{cat} \tag{32}$$

The factor V_{cat} in the differential mass equations is needed to equalize the dimensions on both sides of the equation. V_{cat} is defined as $\rho_{cat}*(1- \varepsilon_b)$. Herein, ρ_{cat} is the density and ε_b the bed voidage of the catalyst respectively [24]. The used catalyst has a density of 1750kg/m^3 and a bed voidage of 0,4, accordingly V_{cat} is 1050kg/m^3. The catalyst section of the reactor has an inner diameter of 24mm and an outer diameter of 48mm [7]. Consequently the cross section area of the catalyst section is 0.0014m^2.

In these differential equations *r* denotes the reaction rate equations of the three occurring reactions developed by Graaf et al. [21], as described in the literature review by equations 9 - 11. To calculate these differential equations, the fugacity *f* for each component in the gas phase has to be calculated from the mSRK equation of state. Therefore the mSRK equation of state (equation 21) can be rewritten to [23]:

$$Z^3 - Z^2 + (A - B - B^2)Z - AB = 0 \tag{33}$$

The fugacity coefficients of the gas phase are calculated by equation 34. First, the roots of equation 33 have to be found. The largest value of the roots belongs to the gas phase. Applying the value this root in equation 34 gives the fugacity coefficients of the components in the gas phase [23].

$$\phi_i^V = \exp\left(\frac{b_i}{b}(Z-1) - \ln(Z-B) - \frac{A}{B}\left[\frac{2\sum_{j=1}^{n} y_j a_{ij}}{a} - \frac{b_i}{b}\right] * \ln\left(1+\frac{B}{Z}\right)\right) \quad (34)$$

Secondly, the fugacity of each component can be calculated with equation 35. In this equation y_i is the mole fraction of the component:

$$f_i = \phi_i^V * P * y_i \quad (35)$$

The equations above are solved with the MATLAB function mSRK_EoS.m written by Martin Bos. With the calculated fugacity of the components in the gas phase, the five differential mass equations can be solved numerically. The ode15s solver in MATLAB R2014b is used to solve the differential equations over the known catalyst bed length of 72mm. The following the initial conditions are used: Since only H_2 and CO_2 are fed to the reactor, the initial weight fractions are: 0% CO, 25% CO_2, 0% MeOH, 75% H_2 and 0% H_2O. The pressure inside the reactor is 50bar and the desired catalyst temperature and mass flow can be filled in manually.

3.2. Condenser

The catalyst out composition is used to calculate an equilibrium flash in the condenser at a defined condenser temperature. It is assumed that the temperature is constant in the condenser. To calculate the equilibrium liquid and vapor mole fractions, the following equation has to be solved:

$$\phi_i^L * x_i = \phi_i^V * y_i \quad (36)$$

In this equation, ϕ_i^L and x_i are the fugacity coefficients and mole fractions in the liquid and ϕ_i^G and y_i the fugacity coefficients and mole fractions in the vapor phase. Therefore, the weight fractions have to be converted into mole fractions. The equation is solved with the MATLAB function Fun_FlashPT.m written by Martin Bos. This function is used to do a flash calculation with respect to the phase equilibrium using the fmincon.m solver in MATLAB. In addition to the vapor mole fractions leaving the catalyst bed, this function needs two starting vectors of an approximation of the vapor and liquid mole fractions of the components after the flash and a defined vapor fraction as input. The function fmincon.m is used to find the minimum of the function Fun_FlashPT.m The resulting output represents the equilibrium liquid and vapor mole fractions after the flash at a given pressure and condenser temperature.

3.3. Addition feed gas to recycle gas stream

It has to be noted that the reactor operates in a gas in liquid out operation mode, as has been described in the literature review. In order to maintain a steady state of mass inside the reactor, the amount of mass that is leaving the reactor as liquid, the product condensate, has to be replaced by an equal amount of mass by the feed gas.

From the resulting liquid equilibrium mole fractions calculated by the condenser model, the mass of the liquid leaving the reactor is determined and the same amount of gas has to be added. The remaining vapor is internally recycled and is fed together with the amount of added feed gas to the catalyst bed as can be seen in Figure 10. This cycle is repeated until the mass flow over the reactor is constant and the reactor approaches steady state.

At steady state the productivity at the defined catalyst and condenser temperature as well as mass flow over the reactor is calculated. It has to be noted that in the experiment, the amount of moles in the reactor are constant instead of a constant mass flow. Therefore, the mass flow gives only an approximation of the gas circulation inside the reactor. The results of this model are presented and discussed in the sensitivity studies in the next paragraph. In chapter 5 the sensitivity studies are compared with the experimental results.

3.4. Sensitivity studies

From the performed experiments in this study it is known that when the experiments are performed under natural and low forced convection, the pressure drop over the catalyst bed is too low to be measured. Therefore, it is not possible to calculate the gas circulation rate inside the reactor and thereby the mass flow over the catalyst bed, which is required for the model.

The manufacturer of the catalyst advises a gas hourly space velocity (GHSV) of 3000/h for the optimal operation of the catalyst. Converted to mass flow and the used amount of catalyst, this results in a mass flow of $5*10^{-5}$kg/s.

This value is used together with the catalyst temperatures of 473 - 523K, a condenser temperature of 373K, a reactor pressure of 50bar and a feed gas composition of 25% CO_2 and 75% H_2 as initial conditions in the model to calculate the productivity at the corresponding catalyst out temperature.

The resulting productivities of this model calculation are presented in Figure 11. Since the mass flow in the reactor is unknown, the effect of the mass flow is investigated by calculating the productivity with a factor 0.5 and 2 of the initial mass flow.

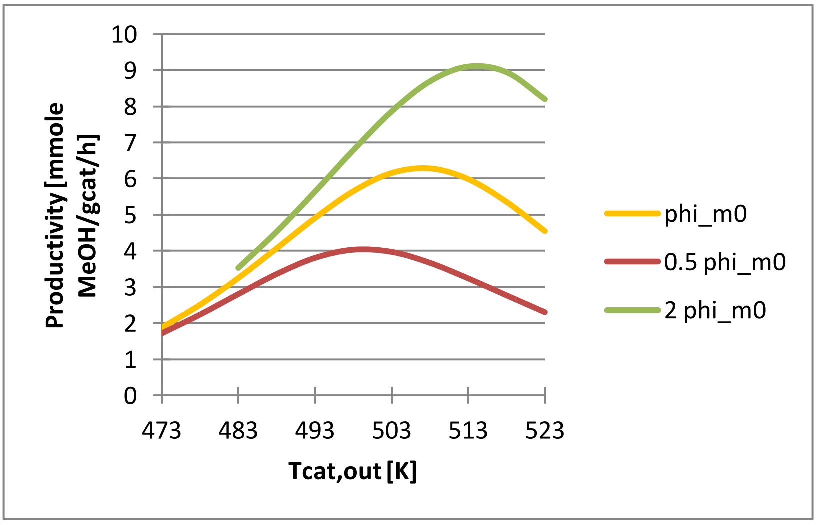

Figure 11: Effect of the mass flow on the productivity

It can be seen in the figure that the productivity increases with increasing mass flow and the maximum in productivity shifts to a higher catalyst out temperature. An increase in mass flow results in a shorter residence time. Therefore, more product is formed and the productivity increases, as long as the kinetics can keep up with the increased mass flow. The effect of the mass flow on the productivity is small at low catalyst out temperature. At high catalyst out temperature, however, the reaction kinetics increase and the reaction approaches the chemical equilibrium productivity.

Next to the mass flow, the used reaction kinetics developed by Graaf et al. (equations 9 – 11) may not match the kinetics in the reactor set up. The reaction rates were developed almost 20 years ago and overtime the catalyst for this reaction has been improved and further developed, so that the reaction kinetics may have changed. Therefore, the effect of the reaction kinetics is investigated by calculating the productivities at the standard reaction rate and a factor 0.5 and 2 of the reaction rates. The results can be seen in Figure 12.

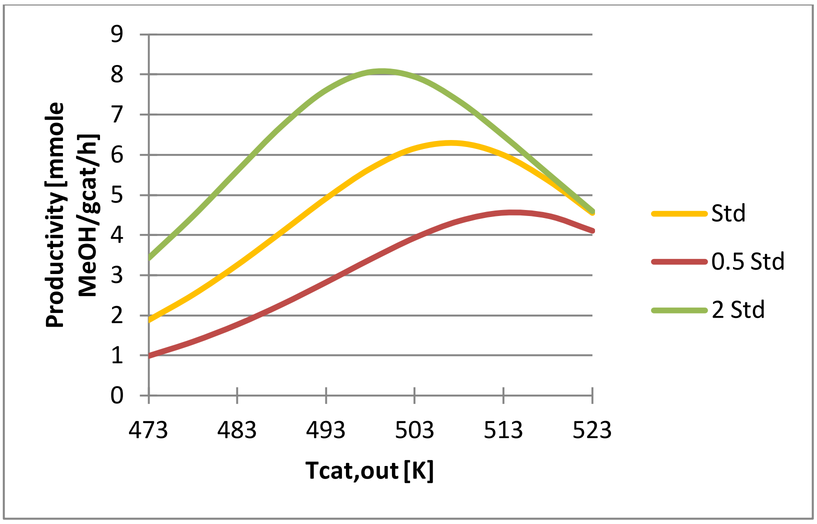

Figure 12: Effect of the reaction rates on the productivity

From the curves in this figure, it follows that an increase in reaction kinetics also results in an increase in productivity. However, the maximum in productivity is shifted to a lower catalyst out temperature. Whereas the effect on the productivity is higher at low catalyst out temperatures is higher, since more product is formed, at high catalyst out temperatures the productivity curves overlap each other, as a result of the fact that the reaction is limited by the chemical equilibrium.

Finally, also the influence of the condenser temperature on the productivity is investigated because it is known that the lower the condenser temperature, the higher the productivity is. The productivities for the condenser temperatures of 333K, 373K and 393K are calculated with advised mass flow and the reaction kinetics developed by Graaf et al. with the model and presented to the corresponding catalyst out temperature in Figure 13.

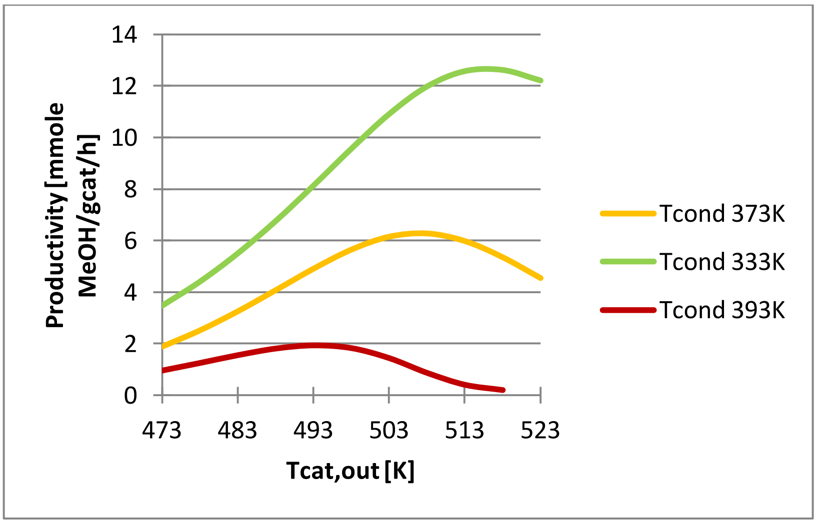

Figure 13: Effect of the condenser temperature on the productivity

This figure shows the expected result: The lower the condenser temperature, the higher the productivity. This is caused by the fact, that at a lower condenser temperature, a larger fraction of the product vapors condensates and thereby, the chemical equilibrium is shifted to the products side. Again, the maximum is shifted to higher catalyst out temperatures due to the fact that the reaction rates increase with temperature.

In chapter 5.3., the calculated model results are compared to the experimental results, which are presented in chapter 5.1..

4. Experimental

In this chapter, first the experimental setup and the activation procedure for the catalyst are described. Then, the operation mode of the reactor setup is introduced, followed by how the measurements are being performed.

4.1. Experimental setup

In this study the same reactor setup, feed gas and catalyst are being used as in the study of Bos [7]. A schematic overview of the reactor setup is given in Figure 14. The reactor consists of a catalyst section (b) at the bottom and a condenser section (d) at the top. In order to maintain a constant pressure in the reactor, a buffer vessel (a) with a volume of 3,8L for the feed gas has been installed.

The feed gas can be fed to this buffer vessel to a maximum pressure of 100bar. The pressure in the buffer vessel is measured by a pressure indicator (PI-1) [GE Druck, Unik PTX-5072-TB-A1-CA-H1-PA, 0-100bar]. The pressure inside the reactor is regulated by a pressure reducer (PCV) between the buffer vessel and the reactor. The reactor pressure is measured by a pressure indicator (PI-2) [GE Druck, Unik PTX-5072-TB-A1-CA-H1-PA, 0-250bar].

This catalyst section (b) of the reactor has an inner diameter of 24mm and an outer diameter of 48mm. The length of this section is 72mm. The catalyst that has been used is a commercial $Cu/ZnO/Al_2O_3$ catalyst (CP-488) provided by Johnson Matthey. It is formed as cylindrical pallets with a 6mm diameter and 5mm length. These pallets are placed in the annular spacing.

The catalyst section is surrounded by a temperature controlled oven (h) [Eurotherm, 2132]. The current to the oven is measured by a current indicator (CI-1) [Phoenix Contact, MACX MCR-SL-CAC-5-I-UP]. The gas temperature at the inlet (TI-3) and outlet (TI-2) of the catalyst section is measured by K-type thermocouples [B+B sensors]. A differential pressure indicator (dP-1) [GE Druck, LPM-9481] is installed to measure the pressure drop over this section. The reactor setup is located in a cold environment. In order to prevent condensation in the pressure lines to the pressure indicator, the lines are packed in a tracer.

A 38mm turbocharger fan (c) is installed in the bottom of the reactor to ensure gas circulation inside the reactor. It draws the recycle and feed gas from the top through the middle of the reactor to the bottom and pushes the gas up through the catalyst bed. The fan is powered by a 30W magnetic coupled motor (M) to ensure a gas-tide power transmission.

The top part of the reactor is the condenser section. The condenser (d) is placed in the inner part of this section. Basically, the condenser is a spiral shaped copper tubing. Through this tubing water is circulated. The temperature of the water is regulated by a water bath (g) [Julabo F34-HE]. The gas temperature of the condenser inlet (TI-5) and outlet (TI-4) are measured by K-type thermocouples [B+B sensors]. The water inlet (TI-7) and outlet temperature (TI-6) of the condenser is measured by K-type thermocouples [B+B sensors]. The water circulation flow is measured by a flow indicator [POM B.I.O-Tech Becker 52.01 in combination with Red Lion IFMA 0035].

The condensed gas, the liquid product of the reaction, is collected inside the reactor in a collection cup. This cup has an approximate volume of 6mL. The liquid product is tapped (V-3) from the reactor to the collection bucket (e) outside the reactor.

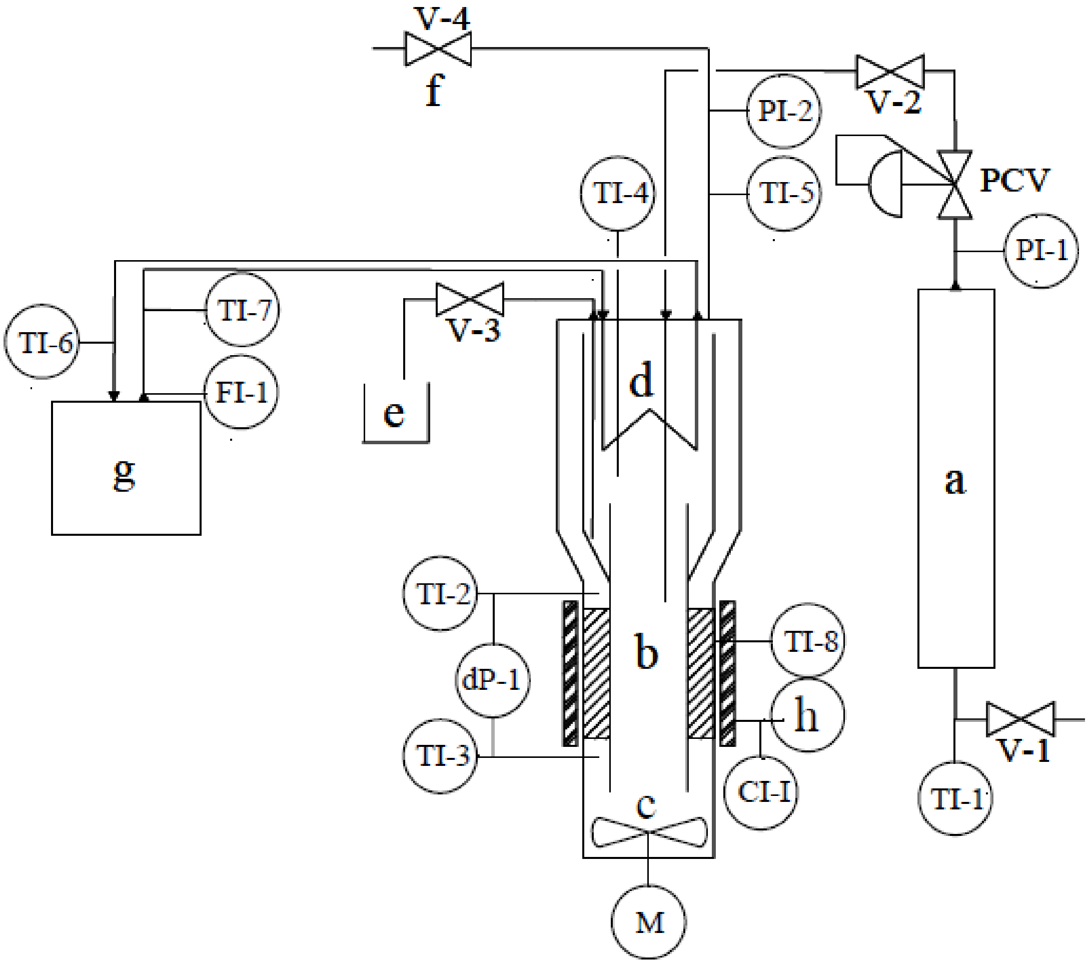

Figure 14: Schematic overview of the reactor set-up: (a) buffer vessel, (b) catalyst section (annulus), (c) fan, (d) cooler, (e) liquid outlet, (f) purge, (g) water bath, (h) oven temperature controller, (TI) temperature indicator, (PI) pressure indicator, (CI) current indicator, (dP) differential pressure indicator, (FI) flow indicator, (PCV) pressure control valve and (V) valve [7].

4.2. Catalyst activation

The annular spacing at the bottom of the reactor is filled with the catalyst pallets and the catalyst is activated according to the procedure provided by the manufacturer. During the activation procedure the catalyst is reduced. This is achieved by first flushing the reactor with nitrogen (N_2) 2L/min at a catalyst out temperature of 433K and pressure of 2bar to remove oxygen (O_2) and water. After flushing, a small amount of hydrogen (H_2) 0.2L/min is added and the nitrogen stream is increased to 3L/min. The addition of hydrogen causes an exothermic reaction, causing an increase in the catalyst out temperature, when the exotherm is passed, the catalyst out temperature decreases. The hydrogen flow is increased to 0.5 L/min and nitrogen flow lowered to 2.5 L/min. After the exotherm passed again, the catalyst out temperature is set to 513K and the reactor is flushed continuously for 2 hours. Then the nitrogen flow is turned off and the reactor is cooled down and is stored under a reducing environment of pure hydrogen.

4.3. Operation

Before an experiment, the buffer vessel is filled with feed gas from the gas bottle and the reactor is flushed with 8bar of feed gas. The feed gas for this experiment is pre-mixed mixture of 25% CO_2 and 75% H_2 obtained from Praxair, the Netherlands. After purging, the reactor is pressurized and heated.

The catalyst outlet temperature is regulated by the temperature of the oven. The condenser is turned on and the condenser outlet temperature is controlled by the flow and by the temperature of the cooling water. For the experiments under forced convection, the fan is turned on and the speed is controlled by the supplied voltage. For experiments under natural convection, the fan is kept off.

The experiments are performed in a semi-continuous mode. This means a continuous amount of feed gas is fed from the buffer vessel to the reactor in order to maintain a constant reactor pressure. This is necessary because the pressure inside the reactor will decrease due to the reaction and the condensation of water and methanol. In order to prevent overflow of the collection cup, the condensate is tapped from the reactor into the collection cup at every two bar of pressure drop in the buffer vessel. After having completed an experiment, the reactor is cooled down and depressurized to 2bar. The fan is turned on and the reactor is flushed with hydrogen for 10 minutes. After flushing, the purge is closed and the reactor is stored under a hydrogen pressure of 5bar, so that the catalyst is in a reducing environment to prevent oxidation.

4.4. Measurements

Firstly, the experimental temperature limitation of the reactor set up has to be determined. Since the heat duty of the oven is limited, the maximum achievable catalyst out temperature by a constant condenser temperature of temperature 383K and constant pressure of 50bar is determined. Secondly, the temperature of the condenser temperature is lowered to 373K in order to investigate whether the catalyst out temperature changes.

As the limitation is known, two series of experiments are being performed. In the first set of experiments, the catalyst out temperature varied between 473 and 523K within the experimental limitations of the reactor setup, whereas the condenser temperature and the fan speed are kept constant at 373K and 2V respectively to study the effects of the catalyst temperature under forced convection. In the second set of experiments, the fan is turned off and the experiment is repeated with the same catalyst out temperatures and condenser temperature to study the effect of the catalyst temperature under natural convection. In both sets, the reactor pressure is kept constant at 50bar.

The productivity of the reactor is measured by the liquid production per unit of time. The productivity is determined over a minimum of 5 condensate samples under stable temperature conditions. The composition of the liquid product is analyzed afterwards in IR absorption measurements. The calibration curves of water and methanol are obtained by injecting pure water and methanol in the IR spectrometer. The liquid product samples are compared to these curves.

The energy efficiency is defined by the energy output, the amount of energy which can be obtained from the produced methanol, divided by energy input, the energy which is used by the oven to heat the catalyst section of the reactor as can be seen in equation 37. To make the energy efficiency dimensionless the quotient has to be multiplied by the mass of the catalyst.

$$E_{eff} = \frac{Productivity * HHV(MeOH)}{Q_{oven}} * m_{cat} \tag{37}$$

5. Results and discussion

The experimental results are presented in this chapter. All the raw data of the experiments including the set points are shown in Appendix A. It has to be noted that in this study only the effect of the catalyst out temperature on the productivity and the energy efficiency under natural and low forced convection (fan speed 2V) of the reactor setup is investigated. For both cases the reactor pressure is kept constant at 50bar and the condenser outlet gas temperature is regulated at 373K.

The influence of water on the used catalyst has not been studied in this study. The experiments were only performed with the in previous experiments used commercial $Cu/ZnO/Al_2O_3$ methanol catalyst so that no comparison and statements on the difference in activity and stability in the presence of water on the catalysts introduced in the literature can be made.

To determine the experimental maximal achievable catalyst out temperature, the oven was set to the maximum temperature of 643K and the outlet of the condenser to 383K. At stable conditions, the maximal achievable catalyst out temperature is 522K. Changing the temperature of the condenser to 373K resulted in a maximal achievable catalyst out temperature of 518K. From these results it follows that experiments can be performed up to a catalyst out temperature of 518K.

First, the productivity and energy efficiency of the reactor setup is determined from the performed experiments. Then, the experimental productivity results are compared to the results of the reactor model.

5.1. Productivity

As discussed in the literature review, the productivity is higher at lower condenser temperature. This is why the measurements were performed at a condenser outlet temperature of 373K. The goal of these experiments is to investigate the effect of the catalyst temperature on the productivity and energy efficiency under natural and forced convection. Since the catalyst out temperature is regulated by the oven, the productivity is determined at the catalyst out temperature. The productivity is measured at the catalyst out temperatures in the range of 473 - 523K under a constant pressure of 50bar for both cases.

The productivity of the reactor is determined by calculating the slope of the plot from the liquid sample weights over time, for a minimum of five samples, under stable temperature conditions. The resulting productivities at the catalyst out temperatures from 473K to 523K under natural and forced convection are shown in Figure 15.

As can be seen in Figure 15, for natural convection there is a maximum in productivity at a catalyst out temperature of 503K, while under forced convection, there is an outlier in productivity at a catalyst out temperature of 518K, which is almost 2,5mmole MeOH/gcat/h higher than at 503K. Furthermore, for both cases, the productivity is almost linearly increasing with the catalyst out temperature until a catalyst out temperature of 503K is reached. At catalyst out temperatures above 503K and neglecting the outlier, the productivity seems to flatten out to a constant level, with a productivity of 5mmole MeOH/gcat/h. This might indicate that the condenser has a limiting role in this reactor set up.

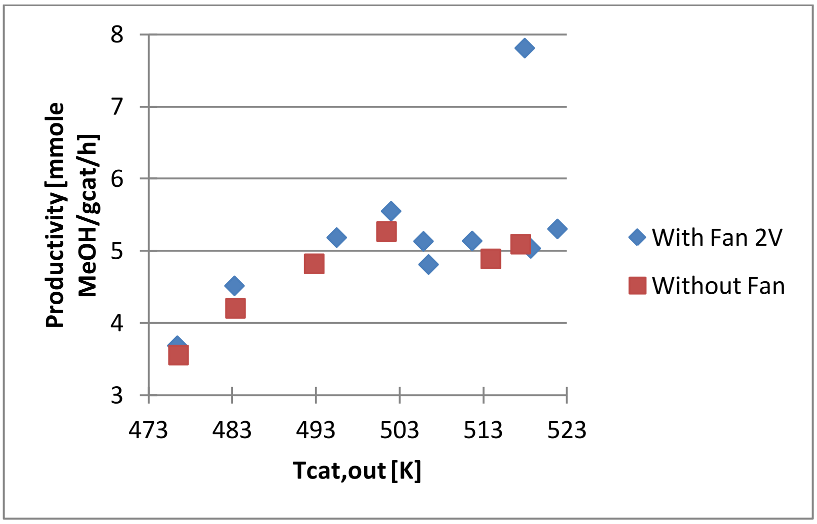

Figure 15: Measured productivities at Tcat,out with Tcond ≈ 373K

In order to find an explanation for this high productivity at a catalyst out temperature of 518K, the set points of the experiments are compared. It is seen that a lower water temperature and lower water flow rate for the condenser are used to maintain the condenser outlet temperature at 373K. Instead of a water temperature of around 333K, the water temperature was 316K during the experiment.

Besides that, the outlier occurred under forced convection. Previous research revealed that the fan speed has an effect on the productivity.

From the literature it is known that a lower condenser temperature leads to a higher productivity. Because of the fact that the temperature of the condenser is measured in the mixed gas phase at the condenser outlet, it is possible that the temperature inside the condenser is lower than the measured temperature and therefore more product will condensate as expected.

Finally, it has to be noted that the experiment of the outlier productivity was the first experiment performed after the activation of the catalyst. The resulting high productivity may be caused by a startup effect of the catalyst. The influence of these factors on the productivity is discussed in the next paragraphs.

5.1.1. Temperature of the cooling water

The effect of the water temperature in the condenser on the productivity is investigated at a catalyst out temperature of 503K and a condenser outlet temperature of 373K. The productivity is measured at three different water temperatures: 316K, 326K and 330K.

The resulting productivities are presented in Figure 16 a).This figure shows a remarkable result. The literature, as discussed above, sets out that a lower condenser temperature results in a higher productivity. However, this figure shows a completely contrary result to the expectation raised by the literature: the productivity is lower at a lower water temperature.

In order to control the condenser out temperature, not only the water temperature can be varied but also the flow rate. At lower water temperatures, lower water flow rates are required to maintain the condenser outlet temperature at 373K as a constant cooler duty is needed. Hence, the water temperature alone does not have the ability to increase the productivity of almost 2,5mmole

MeOH/gcat/h. The water temperatures and the corresponding flow rates are used to calculate the cooler duties, which are the withdrawn energies of the gas stream. The corresponding cooler duties are presented in Figure 16 b). It is immediately apparent that the lower productivity at the lower water temperature is caused by a lower cooler duty. This leads to the conclusion that the temperature of the cooling water did not caused the outlier productivity.

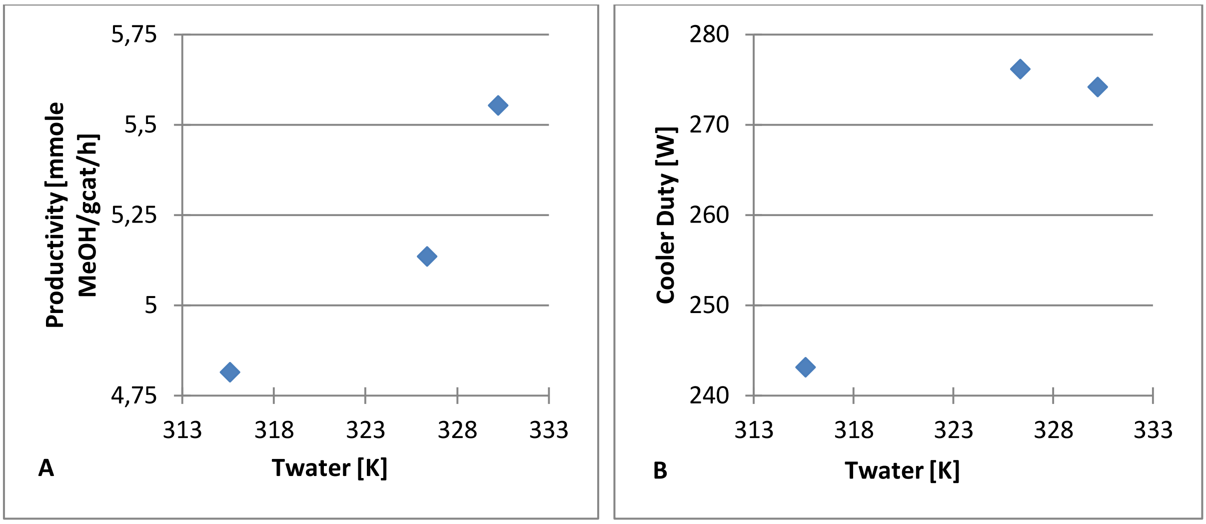

Figure 16: a) Productivity at the water temperature in the condenser b) Corresponding cooler duty at the water temperature in the condenser. Both at a catalyst out temperature of 503K and condenser outlet temperature of 373K and a fan speed of 2V

5.1.2. Fan speed

Another possible explanation for the outlier experiment is that the fan speed may be different than the expected 2V during the experiment. The fan may have faltered during the experiment. This assumption is based on the fact that the current on the fan control display had a constant value, whereas it alternated when the fan rotates. Based on Bos [7] research, it is known that at a fan speed of 1V the productivity is higher than at 2V. Bos measured the productivity at a catalyst out temperature of 473K and a condenser outlet temperature of 363K at different fan speeds. It has to be mentioned that the measurements in this study were performed at different conditions. In this experiment, the catalyst out temperature was about 519K and the condenser outlet temperature of 373K.

In order to verify the hypotheses of a faltering fan, the effect of the fan speed on the productivity is investigated. The productivity is measured at fan speeds of 0V, 1V, 2V and 3V with the same set points as in the original measurement. The resulting productivities are presented in Figure 17. In this figure, the productivity against the fan speed of the original measurement is represented by the red point and the new measured productivities with blue points respectively.

In contrast to the results of Bos, this figure shows a maximum in productivity at a fan speed of 2V instead of 1V. Whereas the results of Bos show a sharp maximum between 0 and 3V, this curve is almost flat. Furthermore, the productivity at 0V and 1V is lower than at 2V. This means that when the fan faltered during the experiment, the productivity would have to be lower. Therefore, faltering of the fan cannot be the cause of the outlier in productivity.

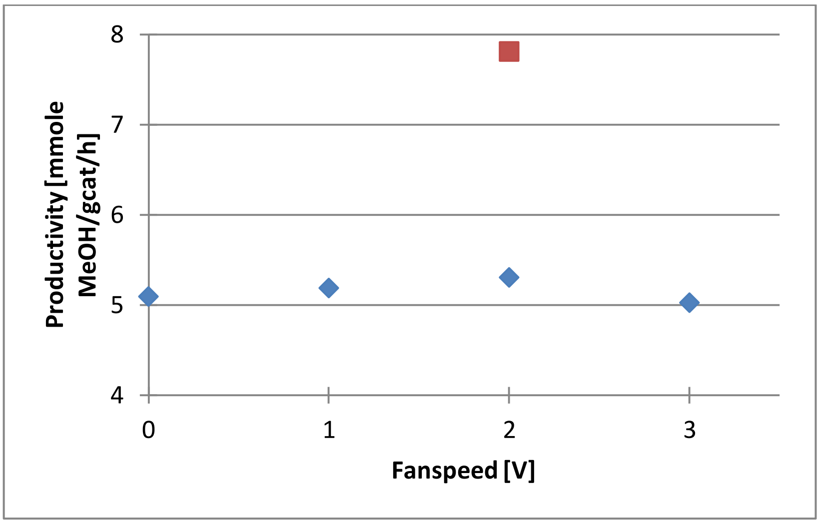

Figure 17: Productivity at fan speed with sp oven 643K, Twater 318K and flow 200 mL/min

5.1.3. Condenser temperature

As mentioned earlier, it is known that the lower the condenser temperature is, the higher the productivity is. Due of the fact that the temperature of the condenser is measured in the gas phase at the condenser outlet below the actual condenser it is possible that the temperature inside the condenser is actually lower than the measured temperature. Therefore, the effect of the condenser outlet temperature on the productivity is investigated.

The productivities are measured at three different condenser outlet temperatures, 363K, 373K and 383K at a catalyst out temperature of 516K under forced convection. The resulting productivities corresponding to the condenser outlet temperatures are represented in Figure 18. In this figure, the red point represents again the outlier measurement of the original experiment. Indeed, the blue points in this figure indicate that the lower the condenser outlet temperature, the higher the productivity is. However, the increase in productivity with a decrease in condenser outlet temperature is small. A decrease of 20K results in an increase of productivity of 1 mmole MeOH/gcat/h. Following this trend, the condenser outlet temperature has to be about 323K to reach a productivity of 7,5mmole MeOH/gcat/h.

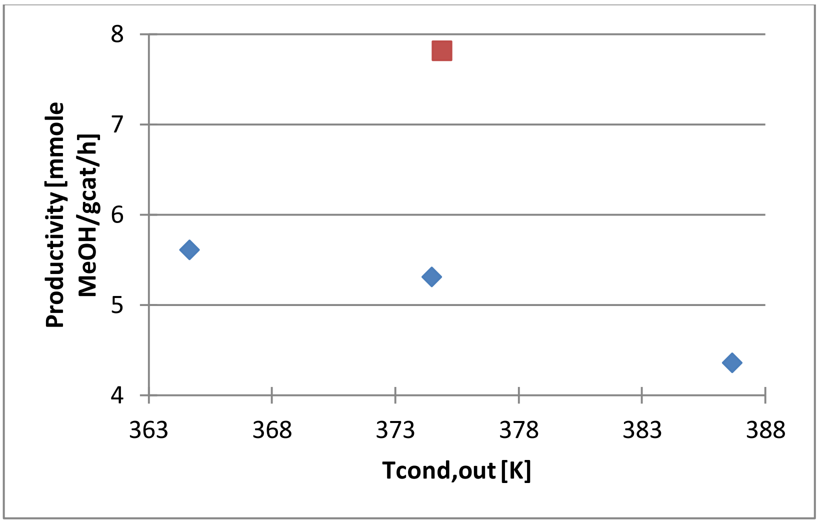

Figure 18: Productivity at Tcond,out with sp oven 643K and fan 2V

Despite the fact that the actual condenser temperature could be lower than the measured temperature in the gas phase at the condenser outlet, a temperature difference of 50K between the actual and measured outlet temperature is not expected. Therefore, it can be concluded outlier productivity was not caused by a lower condenser temperature.

5.1.4. Startup effect of the catalyst

The experiment of the outlier productivity was performed after the activation of the catalyst. During the activation the catalyst is reduced. It may be possible that the reduction of the catalyst was not complete during the activation. Therefore, the catalyst is may be further reduced during the experiment. During this reduction water is produced and generating a faulty productivity based on the condensate mass. To investigate the startup effect of the catalyst the compositions of the liquid samples are analyzed with IR absorption spectrometry. If this hypothesis is true, the amount of water should be higher in the liquid samples of the first experiment performed after the startup of the reactor than in the liquid samples of the experiments performed in later experiments.

Based on the literature, the expectation is raised that only methanol and water are present in the liquid samples. To determine whether methanol and or water are present in the liquid samples, the calibration curves of methanol and water are needed. Therefore, the absorbance of pure methanol and water are measured and the calibration curves are constructed. The calibration curves of pure methanol and water are shown in Figure 19. In this figure, the blue line belongs to water and the red line to methanol.

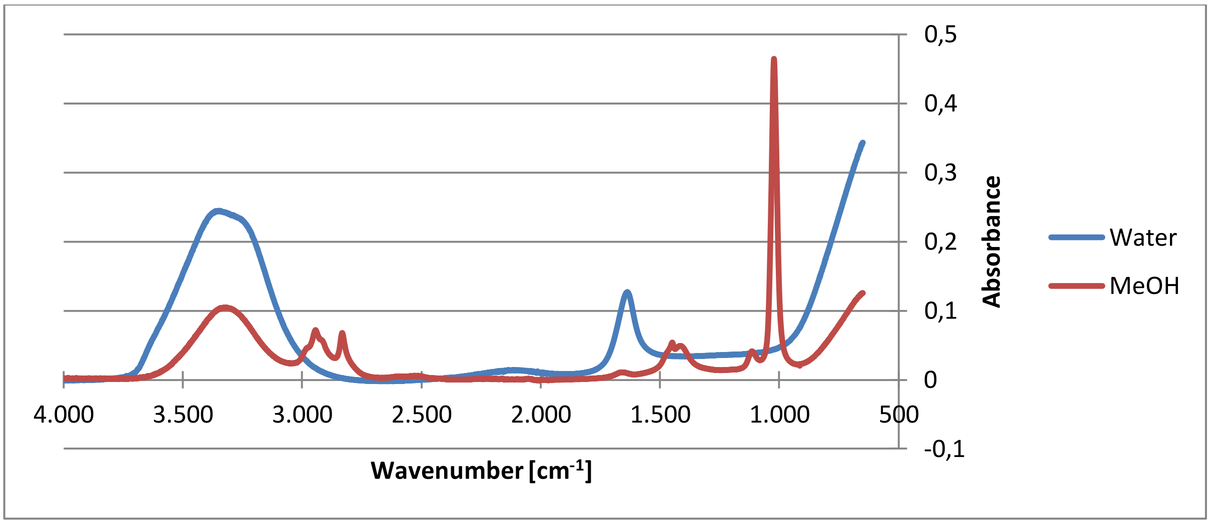

Figure 19: Calibration spectra Water and Methanol

Water shows two absorption peaks: one broad large OH peak at a wavenumber of 3345cm^{-1} and a sharp small OH bending peak at a wavenumber of 1638cm^{-1}. Methanol has seven peaks: Like water, it has a broad OH peak at a wavenumber of 3316cm^{-1}. The two small sharp peaks at wavenumber of 2944cm^{-1} and 2832cm^{-1} indicate CH sp^3 bonding. The three small peaks at wavenumbers of 1449cm^{-1}, 1404cm^{-1} and 1117cm^{-1} determine a CH3 group. The large sharp peak at a wavenumber of 1073cm^{-1} identifies a single CO bonding.

To determine if more water is present in the liquid samples of the first experiment the IR absorbance curves of the liquid samples are compared to the absorbance curve of the liquid sample from the reproducing experiment. The resulting spectra of these IR absorbance measurements are shown in

Figure 20. Samples 1 to 3 are the first three liquid samples of the first experiment after the catalyst activation. The spectra of the liquid samples of the experiments at a catalyst out temperature of 519K and a condenser outlet temperature of 373K under forced convection with a fan speed of 2V are represented by Productivity 8 and Productivity 5 for the high productivity outlier and the productivity of the reproducing experiment respectively.

As can be seen in Figure 20, all five liquid samples lay between the calibration curves of water and methanol. Furthermore, no additional peaks are present in the IR absorption spectra. The spectrum of Sample 1 lies above the spectra of the other samples at the OH peak. This means that the first liquid sample after the catalyst activation contains a bit more water than the subsequent samples. Strikingly, the spectra of Productivity 8 and Productivity 5 overlap each other, which results in the fact that they have the same composition. Therefore, it can be concluded that outlier productivity cannot be caused by the startup effect of the catalyst, since there is not more water in the liquid sample, and that the measured productivity is correct.

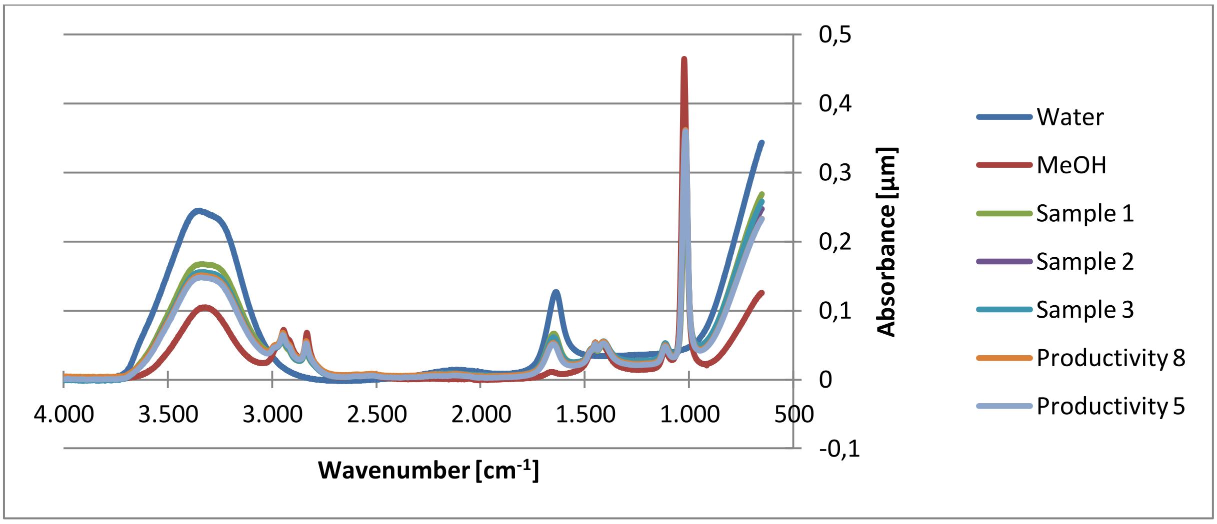

Figure 20: Spectra from the first three liquid samples, the measurement with the outline productivity of 8 and the reproducing measurement with resulting productivity of 5

The influence of the water temperature of the condenser, fan speed, condenser temperature and startup effect of the catalyst on the productivity has been investigated. However, these investigations give not an explanation for the outlier measurement. The results excluding the outlier productivity show that the productivity of the reactor setup increases almost linearly with the catalyst out temperature until a temperature of 503K and then remain constant at productivity of 5mmole MeOH/gcat/h with increasing catalyst out temperature. Since the highest productivity for both forced and natural convection is measured at a catalyst out temperature of 502K, this seems to be the optimal catalyst out temperature by a condenser out temperature of 373K. This result will be compared with the calculated results from the model at the end of this chapter.

5.2. Energy efficiency

As described in the previous chapter, the energy efficiency is calculated by equation 37. In this study, the mass of the catalyst in the reactor is 72,4g. The higher heating value of methanol was found in literature and has a value of 720kJ/mole [25].The energy efficiency at varying catalyst out temperatures, with a constant condenser outlet temperature of 373K for both forced and natural convection is investigated for the reactor setup.

Figure 21 a) shows the required energy input, the needed oven duties, to reach the required catalyst out temperatures. The trend in this figure is as expected: The higher the catalyst out temperature, the more energy the oven requires to heat the gas stream to this temperature. With these oven duties the energy efficiencies at the corresponding catalyst out temperatures are calculated. The resulting energy efficiencies under forced and natural convection at a condenser outlet temperature of 373K are presented in Figure 21 b). It can be seen that both curves for natural and forced convection show a clear maximum of energy efficiency at a catalyst out temperature of 502K. At this temperature the productivity is the highest as is shown above. At higher temperatures the productivity remains constant whereas the oven duties increase resulting in a decrease in energy efficiency. The energy efficiency under forced convection is slightly higher because it has a slightly higher productivity than under natural convection.

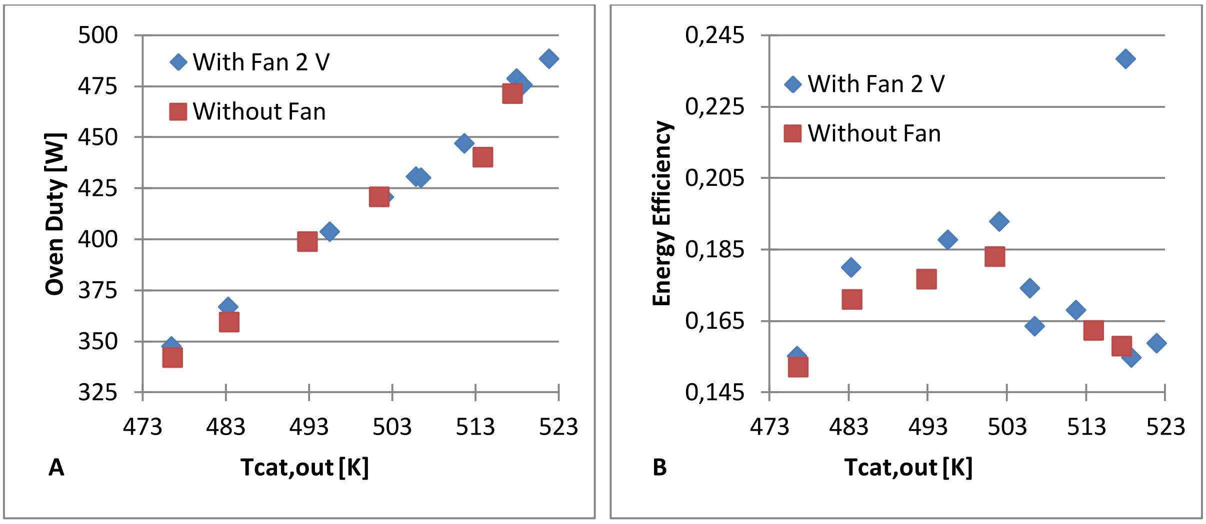

Figure 21: a) Oven duty at the catalyst out temperature. b) Energy efficiency at the catalyst out temperature. Both at a condenser outlet temperature of 373K

Additionally, the energy efficiency at a catalyst out temperature of about 519K with varying condenser outlet temperatures under forced convection is investigated. Figure 22 a) shows the required oven duties in order to maintain the catalyst out temperature of 519K at a fan speed of 2V. In this figure, the red point represents the result of the outlier measurement. Notable is that the lower the condenser outlet temperature, the more energy is required to maintain the catalyst out temperature at 519K. This is due to the fact that the catalyst in temperature is lower at lower condenser outlet temperature. Therefore, more energy is required to heat up the gas again to reach the desired catalyst out temperature.

The resulting energy efficiencies at a catalyst out temperature of about 519K with varying condenser outlet temperatures under forced convection are shown in Figure 22 b). Again, the red point represents the outline measurement. As mentioned earlier, the methanol duty is linked to the productivity. Since the productivity is higher at lower condenser outlet temperature, also the energies delivered by the methanol are. Despite the higher necessary oven duties to maintain the catalyst out temperature at 519K, the energy efficiency is higher at low condenser temperatures due to the fact that the productivity is higher at lower condenser outlet temperatures.

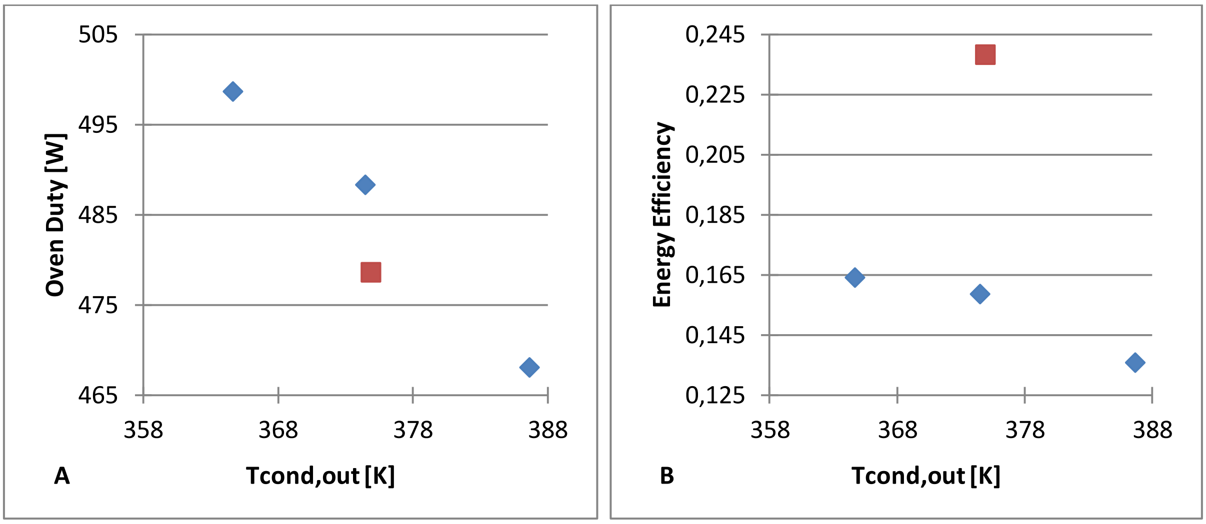

Figure 22: a) Required oven duties to maintain a catalyst out temperature of 519K at different condenser outlet temperatures b) Corresponding energy efficiencies at different condenser outlet temperatures with a catalyst out temperature of 373K

From these results, it can be concluded that under the conditions used in this study, a catalyst out temperature of 502K and condenser outlet temperature of 373K has the highest energy efficiency of 0,193 and 0,183 for forced and natural convection respectively.

5.3. Comparison model with experimental results

The experimental results are compared to the model results from the sensitivity studies in chapter 3.4.. The comparisons are presented in Figures 23 to 25. It is notable that all model results show a clear maximum in the productivity curves over the catalyst out temperature range from 473K to 523K, whereas the experimental results do not. This indicates that a limiting factor is present in the reactor setup. Furthermore, it can be seen that the experimental and model results have the same order of magnitude. However, none of the calculated curves overlaps with the experimental results.

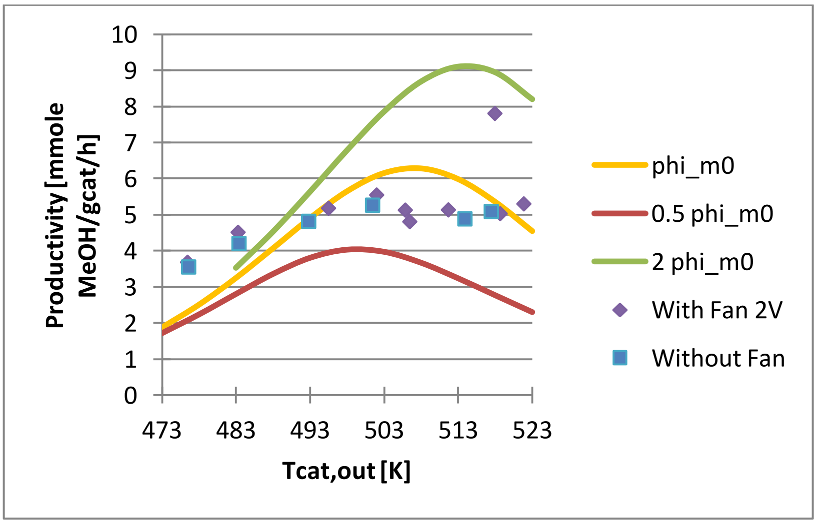

Figure 23: Comparison experimental results with the calculated results at different mass flow rates

By taking a closer look at Figure 23: Comparison experimental results with the calculated results at different mass flow ratesFigure 23, the experimental results at low catalyst out temperatures lie above the curves of the model calculations at different mass flows. As described in chapter 3.4., the effect of the mass flow at low temperatures is only small. At higher temperatures, however, the influence is quite big. As can be seen, at higher catalyst out temperatures, the experimental productivities are higher than the calculated productivities at half the advised mass flow but way lower than the calculated productivities at the double mass flow. From this observation it can be concluded that the assumed mass flow of $5*10^{-5}$kg/s, despite the fact that it has higher productivities, is a fair approach of the mass flow over the catalyst bed.

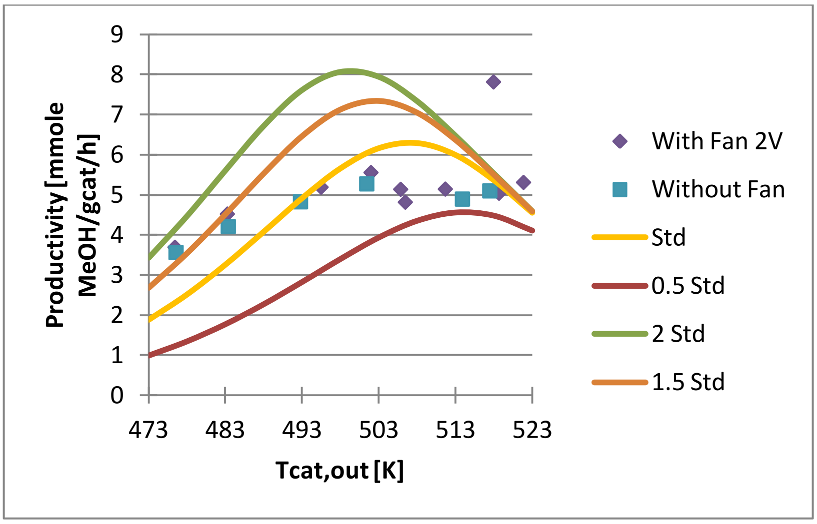

Figure 24: Comparison experimental results with the calculated results at different reactions rates

By comparing the experimental results with the effect of the reaction rates on the productivity, as is presented in Figure 24, it can be observed that the reaction kinetics is higher at low catalyst out temperatures than the developed kinetics by Graaf et al.. It seems that, at low catalyst out temperatures, the experimental productivity corresponds with the productivity of 1.5 times the Graaf reaction rates. However, at higher catalyst out temperatures, this is no longer valid. At the maximum catalyst out temperatures, the experimental productivity is close to the chemical equilibrium productivity.

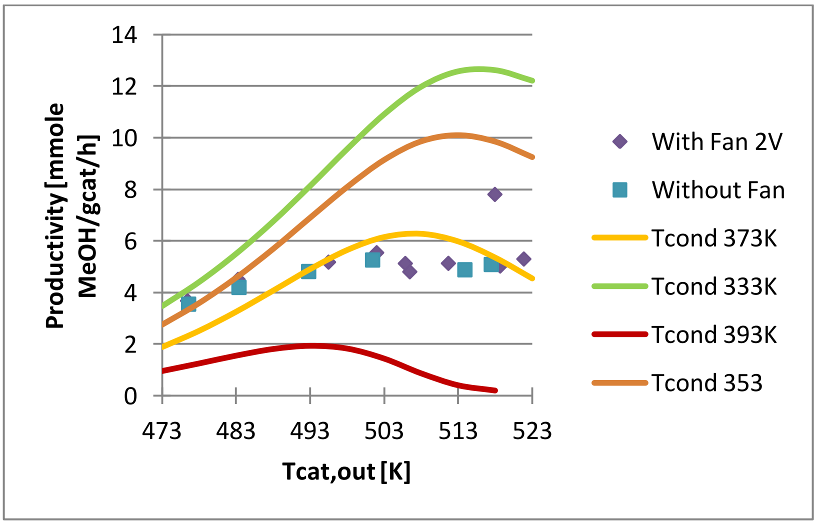

Figure 25: Comparison experimental results with the calculated results at different condenser temperatures

Finally, by analyzing the comparison of the experimental results with the influence of the condenser temperature on the productivity, as is showed in Figure 25, it can be seen that, at low temperatures, the experimental results seem to match the results of a condenser temperature of 353K. Nevertheless, the productivity is almost twice as high at higher catalyst out temperatures. Instead of a strong increase, the experimental productivity increases only slowly. As discussed earlier, the temperature of the condenser is measured in the outlet gas stream. Since most of the experiments were performed with a water temperature of 333K, the productivity at this condenser temperature is also calculated in order to investigate whether the water temperature of the condenser has an effect on the condenser temperature. As can be seen, the productivities at this condenser temperature are higher. Hence, this is not the case in the performed experiment. From these results it concluded that the reactor set up is limited by the condenser at high catalyst out temperatures.

The comparisons of the experimental results with the calculated results show that the model is dependent on more than one variable. It was not possible to determine these variables in this study. To determine the variables more experimental research is required. The recommendations for further research are discussed in the next chapter.

6. Recommendation

For future research, the kinetic and phase equilibrium based reactor model has to be optimized in order to give precise predictions on the performance of the reactor. Therefore, it is necessary to find the discussed unknown variables.

A relation that describes the gas circulation rate inside the reactor is needed. Experiments with sufficient fan speeds can be performed to measure the pressure drop over the catalyst bed. The resulting data on the pressure drop can be used to calculate the gas flow circulation and thereby the mass flow over the catalyst bed.

Furthermore, the results of this study have shown that the temperature over the catalyst bed is not constant. The catalyst in temperatures are much lower than the catalyst out temperatures. The present temperature gradient is not included in the model. This gradient has to be implemented in the model to give a better description of the reactor setup.

Besides that, the used reaction kinetics developed by Graaf et al. (equations 9 – 11) may not match the kinetics in the reactor set up. The reaction rates were developed almost 20 years ago. In the past years, the catalysts for this reaction have been improved and further developed so the reaction kinetics may have changed. Therefore, it is necessary to fine tune the kinetic rates in order to improve and fit the model to the experimental results.

Finally, it has to be noted that in the experimental reactor setup the amount of moles is equal instead of the mass. The usage of the mass flow in the model gives only an approximation of the gas circulation inside the reactor. Therefore, the mass balance over the catalyst bed has to be replaced by the mole balance in order calculate accurate conversions and productivities.

As discussed, the reactor setup is limited by the condenser. The influence of the condenser temperature on the productivity could be further investigated. At a condenser out temperature of 373K, the productivity remains constant after a catalyst out temperature of 503K. Experiments with higher and lower condenser out temperatures will be necessary in order to investigate whether the productivity remains constant at a higher or lower productivity or conversely shows a clear maximum.

In addition to this, the reactor could be operated with another catalyst. Research has shown that catalysts with better properties, such as activity and stability, have already been developed for this reaction. The productivity can be measured and can be compared to the productivity results with the used catalyst in this study. If the productivity is higher or the same productivity is reached at a lower catalyst out temperature, the energy efficiency of the reactor setup is improved.

7. Conclusion

In this study, the effect of the catalyst out temperature on the productivity and the energy efficiency under natural and low forced convection (fan speed 2V), at a constant reactor pressure of 50bar and a constant condenser outlet gas temperature of 373K, of the reactor setup has been investigated.

A simplified mathematical, mass balance based, steady state model has been developed to describe the reactor setup. This model however, can only approximate the theoretical productivity at the catalyst out temperatures, because the gas circulation rate inside the reactor is unknown since no pressure drop over the catalyst bed was too low to be measured under natural and low forced convection. Additionally, the experimental results showed that here is a temperature gradient present over the catalyst bed, in contrast to the assumption that the temperature over the catalyst bed is constant. Therefore, the developed model has to be improved to enhance the prediction of the experimental results.

Whereas the model results show a clear maximum in productivity over the catalyst out temperature range from 473K to 523K, the experimental results show almost a linearly increase in productivity with the catalyst out temperature until a catalyst out temperature of 503K is reached. With further increasing catalyst out temperatures the productivity remains at constant level, with a productivity of 5mmole MeOH/gcat/h. From this result it can be concluded that the reactor setup is limited by the condenser.

The highest experimental achieved productivity of 5,553mmole MeOH/gcat/h and 5,271mmole MeOH/gcat/h for both forced and natural convection respectively, is measured at a catalyst out temperature of 502K.

Due to the fact that the reactor setup is limited by the condenser, it can be concluded that under the conditions in this study, the highest energy efficiency of 0,193 and 0,183 for forced and natural convection respectively is reached at a temperature of 502K.

Therefore, the catalyst out temperature of 502K is identified as the optimal catalyst out temperature by a condenser outlet gas temperature of 373K.

8. References

1. Olah, G.A., A. Goeppert, and G.K.S. Prakash, *Chemical Recycling of Carbon Dioxide to Methanol and Dimethyl Ether: From Greenhouse Gas to Renewable, Environmentally Carbon Neutral Fuels and Synthetic Hydrocarbons.* The Journal of Organic Chemistry, 2008. **74**(2): p. 487-498.
2. Goeppert, A., et al., *Recycling of carbon dioxide to methanol and derived products - closing the loop.* Chemical Society Reviews, 2014. **43**(23): p. 7995-8048.
3. Ott, J., et al., *Methanol*, in *Ullmann's Encyclopedia of Industrial Chemistry*. 2000, Wiley-VCH Verlag GmbH & Co. KGaA.
4. Graves, C., et al., *Sustainable hydrocarbon fuels by recycling CO2 and H2O with renewable or nuclear energy.* Renewable and Sustainable Energy Reviews, 2011. **15**(1): p. 1-23.
5. English, A., et al., *Methanol*, in *Kirk-Othmer Encyclopedia of Chemical Technology*. 2000, John Wiley & Sons, Inc.
6. Jadhav, S.G., et al., *Catalytic carbon dioxide hydrogenation to methanol: A review of recent studies.* Chemical Engineering Research and Design, 2014. **92**(11): p. 2557-2567.
7. Bos, M.J. and D.W.F. Brilman, *A Novel Condensation reactor for Efficient co2 to methanol conversion for storage of renewable electric energy.* Chemical Engineering Journal, (0).
8. Li, C., X. Yuan, and K. Fujimoto, *Development of highly stable catalyst for methanol synthesis from carbon dioxide.* Applied Catalysis A: General, 2014. **469**(0): p. 306-311.
9. Peter Atkins, J.d.P., *Atkins Physical Chemistry*. Vol. 9. 2010: Oxford University Press.
10. Liu, X.-M., et al., *Recent Advances in Catalysts for Methanol Synthesis via Hydrogenation of CO and CO2.* Industrial & Engineering Chemistry Research, 2003. **42**(25): p. 6518-6530.
11. Wu, J., et al., *The stability of Cu/ZnO-based catalysts in methanol synthesis from a CO2-rich feed and from a CO-rich feed.* Applied Catalysis A: General, 2001. **218**(1-2): p. 235-240.
12. Saito, M. and K. Murata, *Development of high performance Cu/ZnO-based catalysts for methanol synthesis and the water-gas shift reaction.* Catalysis Surveys from Asia, 2004. **8**(4): p. 285-294.
13. Lim, H.-W., et al., *Modeling of the Kinetics for Methanol Synthesis using Cu/ZnO/Al2O3/ZrO2 Catalyst: Influence of Carbon Dioxide during Hydrogenation.* Industrial & Engineering Chemistry Research, 2009. **48**(23): p. 10448-10455.
14. Lee, J.S., et al., *A Comparative Study of Methanol Synthesis from CO2/H2 and CO/H2 over a Cu/ZnO/Al2O3 Catalyst.* Journal of Catalysis, 1993. **144**(2): p. 414-424.
15. An, X., et al., *Methanol Synthesis from CO2 Hydrogenation with a Cu/Zn/Al/Zr Fibrous Catalyst.* Chinese Journal of Chemical Engineering, 2009. **17**(1): p. 88-94.
16. Sahibzada, M., I.S. Metcalfe, and D. Chadwick, *Methanol Synthesis from CO/CO2/H2over Cu/ZnO/Al2O3at Differential and Finite Conversions.* Journal of Catalysis, 1998. **174**(2): p. 111-118.
17. Zhang, Y., et al., *A high activity Cu/ZnO/Al2O3 catalyst for methanol synthesis: Preparation and catalytic properties.* Applied Catalysis A: General, 1997. **158**(1–2): p. 105-120.

18. Martin, O. and J. Perez-Ramirez, *New and revisited insights into the promotion of methanol synthesis catalysts by CO2.* Catalysis Science & Technology, 2013. **3**(12): p. 3343-3352.
19. Skrzypek, J., et al., *Thermodynamics and kinetics of low pressure methanol synthesis.* The Chemical Engineering Journal and the Biochemical Engineering Journal, 1995. **58**(2): p. 101-108.
20. Rahimpour, M.R., et al., *Methanol synthesis in a novel axial-flow, spherical packed bed reactor in the presence of catalyst deactivation.* Chemical Engineering Research and Design, 2011. **89**(11): p. 2457-2469.
21. Graaf, G.H., E.J. Stamhuis, and A.A.C.M. Beenackers, *Kinetics of low-pressure methanol synthesis.* Chemical Engineering Science, 1988. **43**(12): p. 3185-3195.
22. Graaf, G.H., et al., *Chemical equilibria in methanol synthesis.* Chemical Engineering Science, 1986. **41**(11): p. 2883-2890.
23. Bennekom, J.G.v., et al., *Modeling and Experimental Studies on Phase and Chemical Equilibria in High-Pressure Methanol Synthesis.* Industrial & Engineering Chemistry Research, 2012. **51**(38): p. 12233-12243.
24. Manenti, F., S. Cieri, and M. Restelli, *Considerations on the steady-state modeling of methanol synthesis fixed-bed reactor.* Chemical Engineering Science, 2011. **66**(2): p. 152-162.
25. P.J. Linstrom, W.G.M. *NIST Chemistry WebBook, NIST Standard Reference Database Number 69, National Institute of Standards and Technology, Gaithersburg MD, 20899, http://webbook.nist.gov*, .

9. Appendix

A. Experimental data and set points

	Experiment	TcatIn [°C]	TcatOut [°C]	TcoolerIn [°C]	TcoolerOut [°C]	TwaterIn [°C]	TwaterOut [°C]	Productivty [mmole/gcat/h]	Preactor [Bar]	Flow [mL/min]	Qoven [W] [W]	Qwater [W]	SP Oven [°C]	SP Fan [V]	SP WB [°C]	SP Flow [mL/min]	Eeff
With fan	141210-0028	190,3	248,6	187,5	**113,7**	59,7	82,3	**4,356**	50,30	163	468,09	252,61	370	2	62	150	0,136
	141210-0028	182,2	245,0	184,4	**101,9**	43,0	64,0	**7,812**	50,12	205	478,64	292,66	370	2	45	200	0,238
	150107-0036-2	168,5	243,3	183,3	**91,7**	30,6	53,6	**5,607**	50,20	202	498,68	317,29	370	2	30	200	0,164
	141211-0029	154,7	**203,4**	159,5	103,5	61,0	80,6	**3,689**	50,09	147	347,38	197,32	292	2	65	130	0,155
	141211-0029	159,6	**210,3**	163,9	104,0	61,1	78,8	**4,519**	50,02	184	366,73	221,99	305	2	65	160	0,180
	141212-0030	164,5	**222,5**	171,5	105,4	58,9	77,4	**5,187**	49,96	197	403,59	249,71	325	2	62	200	0,188
	141217-0033	169,6	**238,7**	182,3	103,2	53,5	69,2	**5,140**	50,28	269	446,86	289,24	345	2	56	250	0,168
	150106-0035	172,5	**245,7**	186,6	104,1	42,9	69,2	**5,037**	50,17	153	475,50	274,65	365	2	45	140	0,155
	141212-0030	169,0	229,0	176,1	105,3	**57,2**	74,4	**5,553**	50,17	233	420,58	274,15	338	2	60	220	0,193
	141217-0033	164,9	232,9	178,7	102,9	**53,4**	70,2	**5,135**	50,14	240	430,60	276,13	340	2	56	220	0,174
	150105-0034	163,9	233,5	179,2	102,7	**42,6**	71,6	**4,814**	49,91	123	430,04	243,10	342	2	45	110	0,163
	150106-0035	172,4	248,9	188,8	101,5	43,0	64,2	**5,307**	50,67	205	488,34	296,93	370	**2**	45	200	0,159
	150107-0036	164,6	248,8	189,3	101,6	42,9	65,3	**5,027**	50,22	204	504,46	312,60	370	**3**	45	200	0,146
	150107-0036	181,5	244,8	186,0	97,7	43,1	63,8	**5,190**	50,15	201	469,78	284,73	370	**1**	45	200	0,161
Without fan	150107-0036-2	182,0	244,5	185,8	97,4	43,1	63,8	**5,095**	50,17	201	471,27	284,99	370	**0**	45	200	0,158
	141215-0031	160,7	**203,6**	159,2	103,1	61,5	80,4	**3,559**	49,86	142	341,89	183,01	295	0	65	140	0,152
	141215-0031	165,7	**210,4**	163,0	103,2	61,8	77,0	**4,207**	49,88	196	359,31	204,34	307	0	65	180	0,171
	141216-0032	170,1	**219,8**	170,0	102,7	59,1	73,5	**4,823**	50,32	248	398,74	243,98	327	0	62	240	0,177
	141216-0032	176,7	**228,4**	175,1	103,5	57,3	72,2	**5,271**	50,28	294	420,67	298,96	342	0	60	250	0,183
	150105-0034	181,3	**240,9**	183,7	102,8	57,0	70,1	**4,891**	50,18	322	440,11	287,94	358	0	60	300	0,162